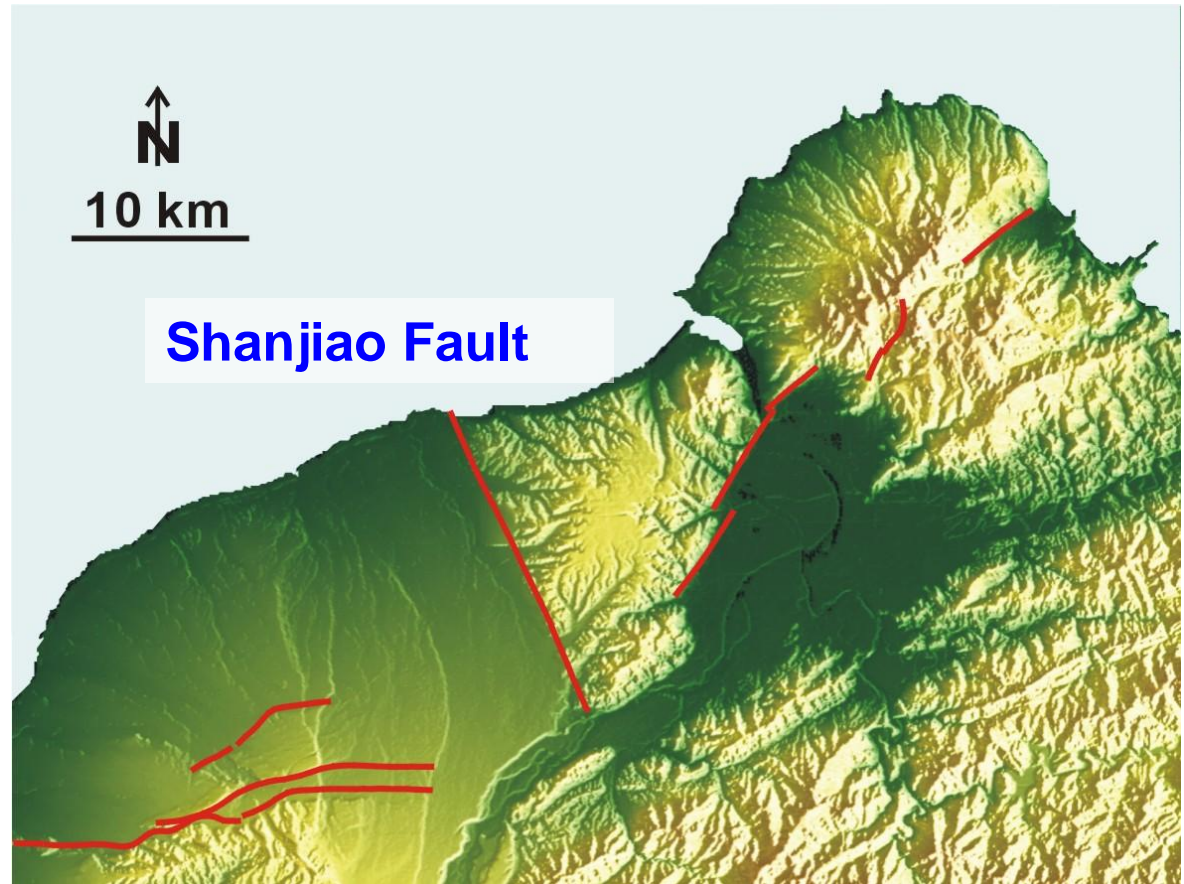


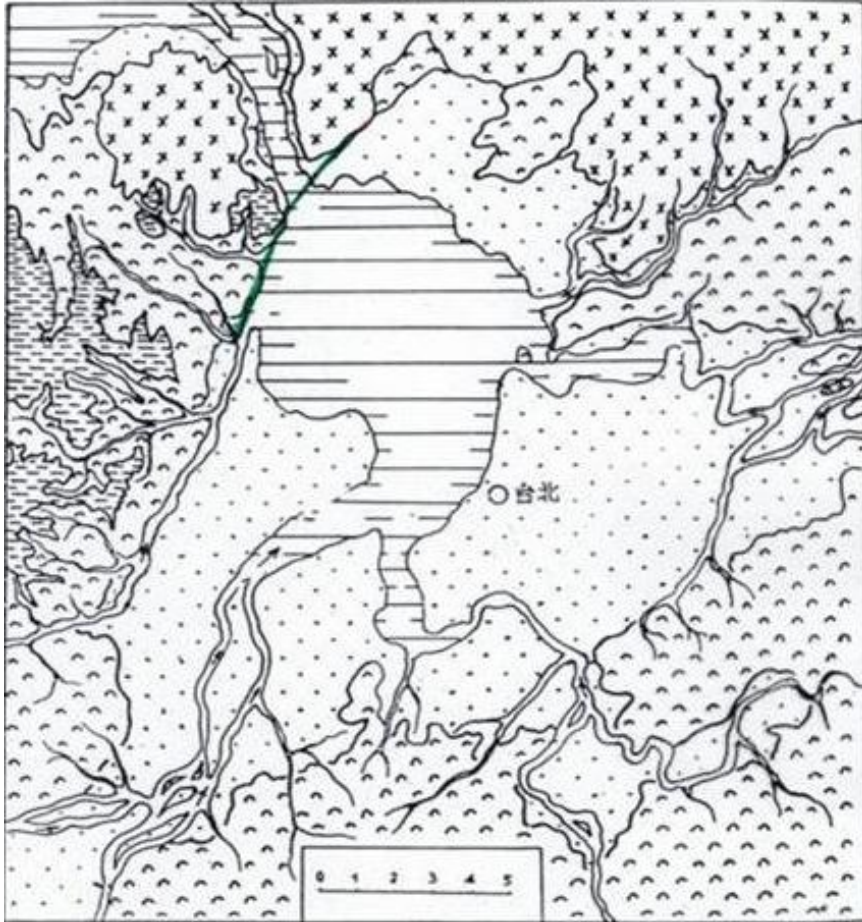
台灣山脈內盆地的成因

張中白

Taipei basin



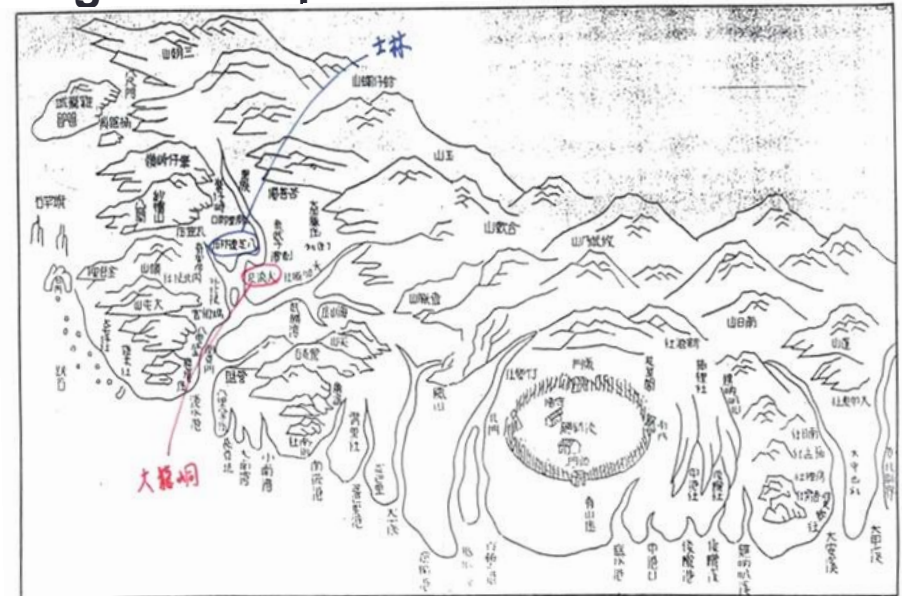
- 243 Km² in area
- Biggest basin in Taiwan
- Most densely populated metropolitan
- Surrounded by active fault
- Triangular in shape



Reconstructed Taipei Lake
 - drew by Lin Chao-Chi, 1960
 - after Yu's record, 1694



Regional map of 1717



Regional map of 1741



觀音山

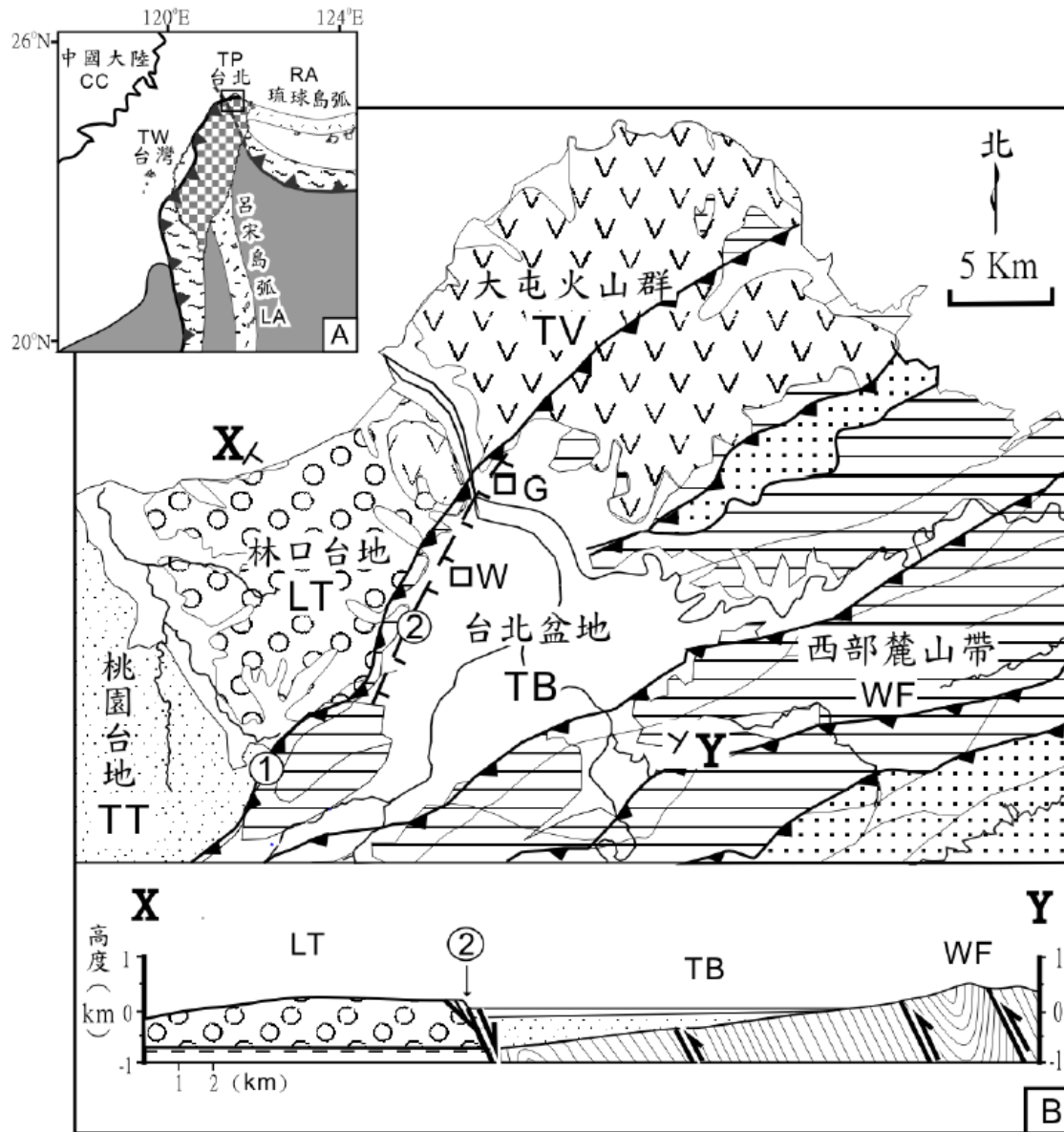
八里分社
(八里鄉龍潭、朱金)

甘答門 (關渡)

麻少翁社
(平林區社子)

淡水

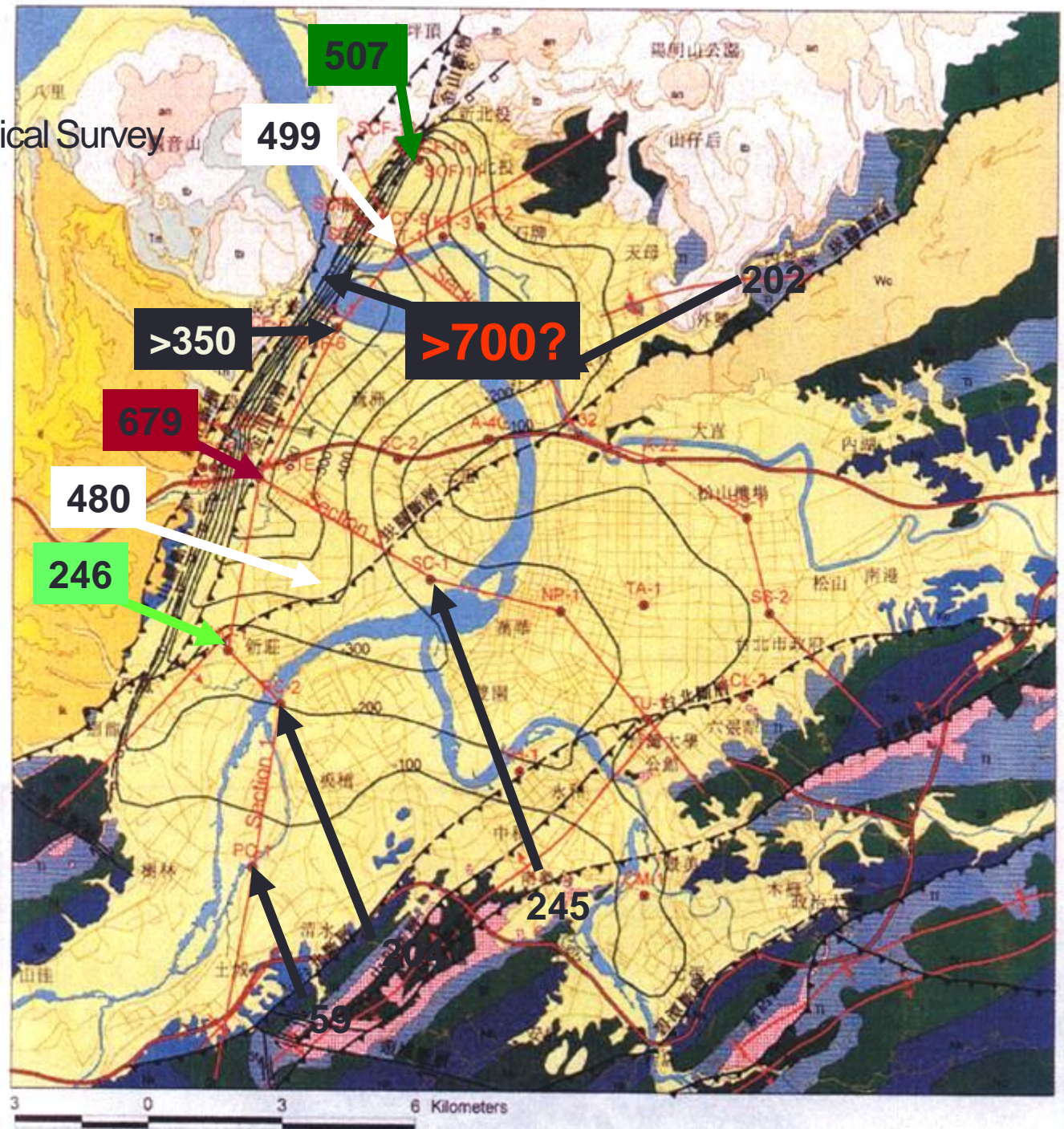
Geological background



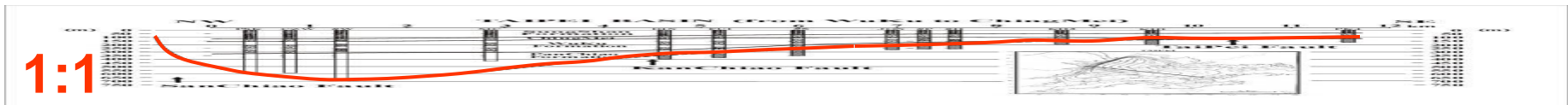
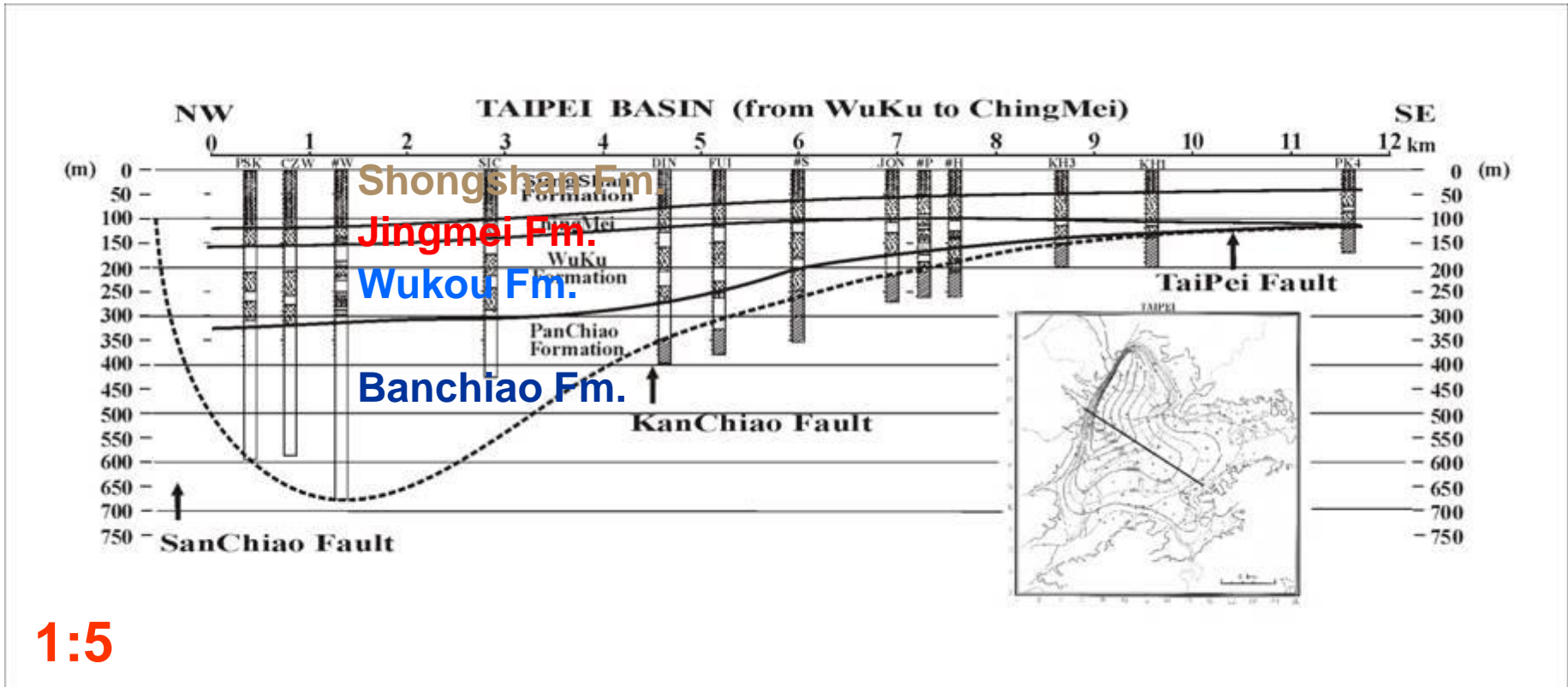
- a** 全新統
- b** 更新統
火山群
- c** 上更新統
- d** 下更新統
- e** 上新統
- f** 中新-
漸新統
- G** 關渡
- W** 五股
- ①** 新莊斷層
- ②** 山腳斷層

Drilling data

after the Central Geological Survey

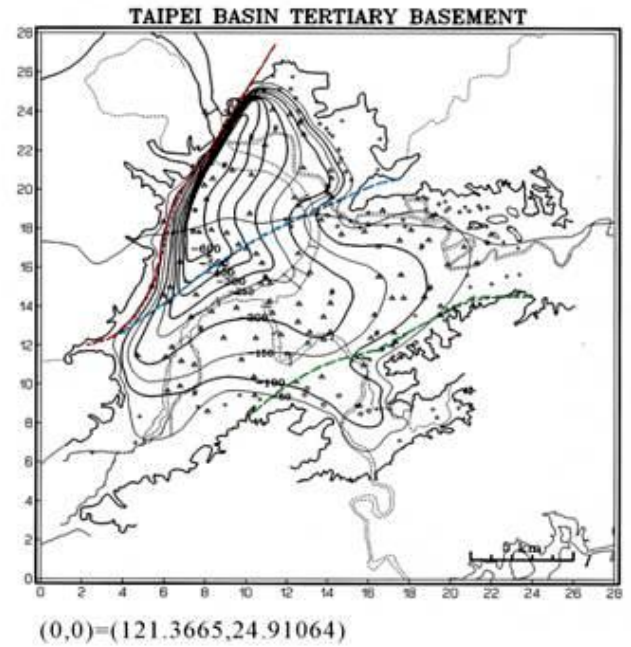
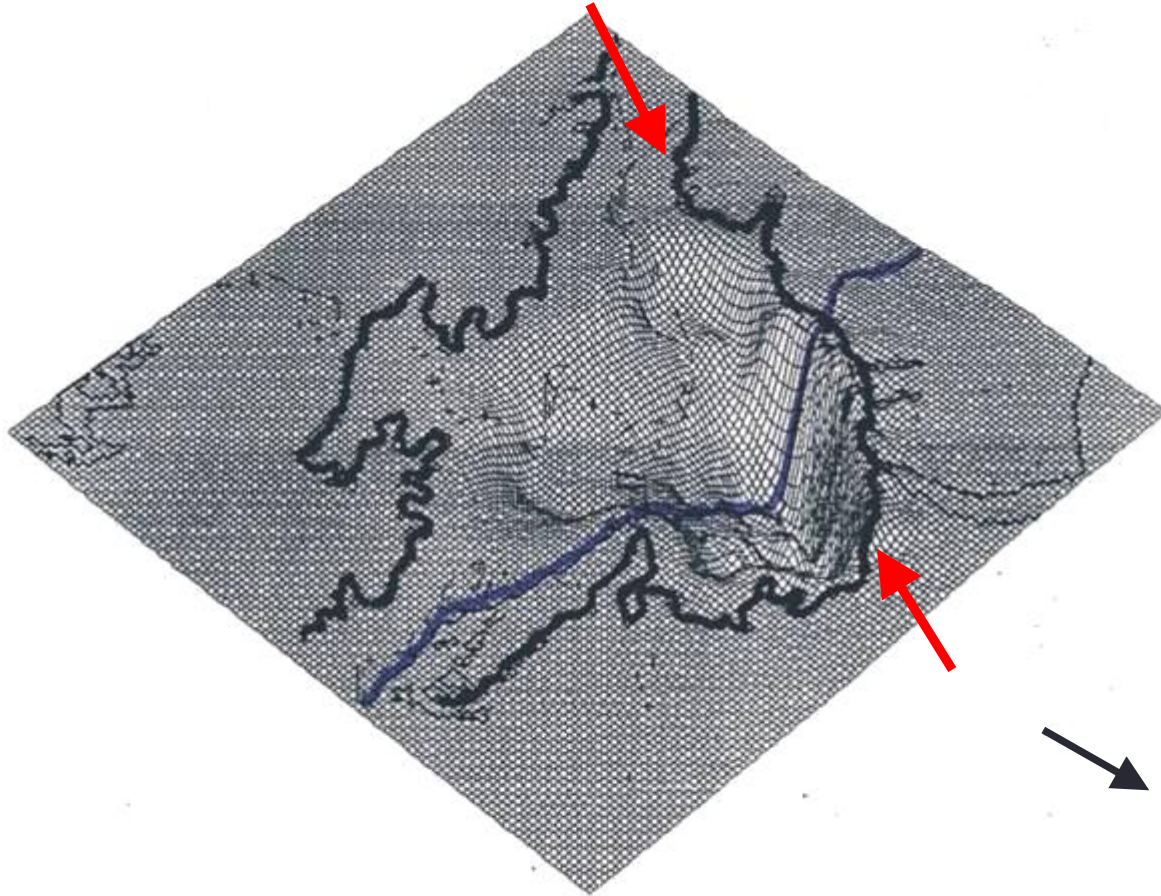


Quaternary Stratigraphical profile cut across the Taipei basin



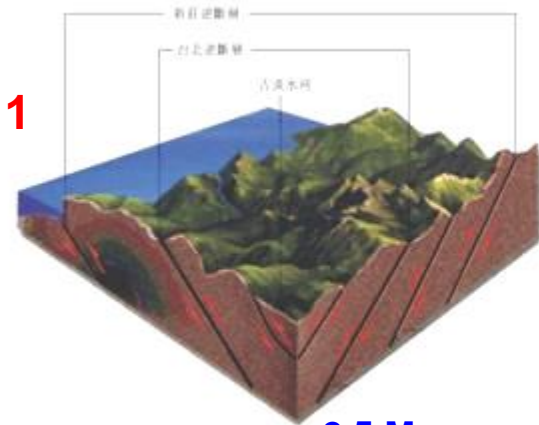
Basement of the Taipei basin

Shanjiao Fault

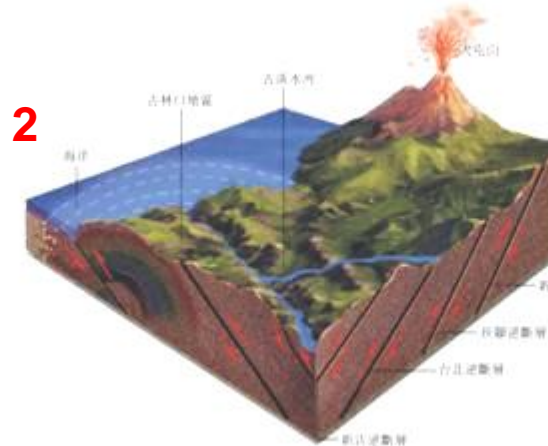


TAIPEI BASIN TERTIARY BASEMENT

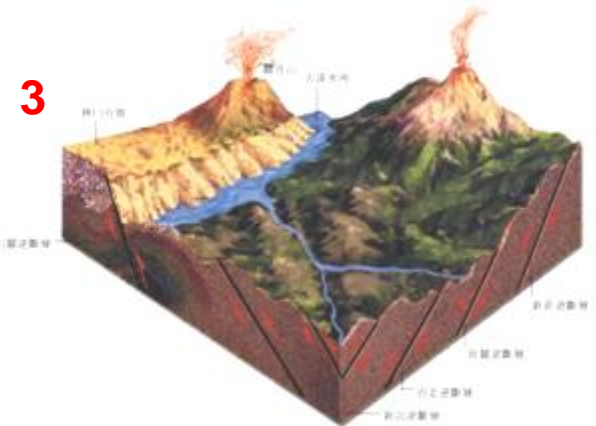
Tectonic evolution of the Taipei basin



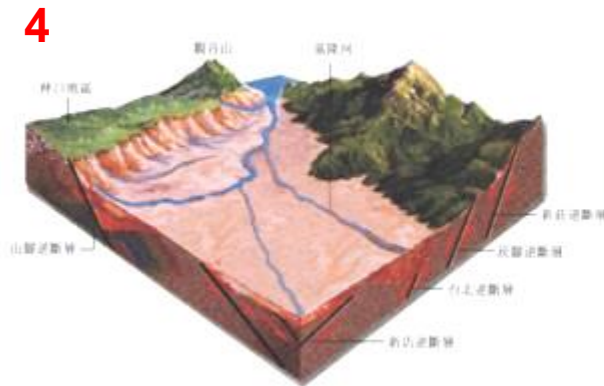
2.5 Ma
Thrusting deformation



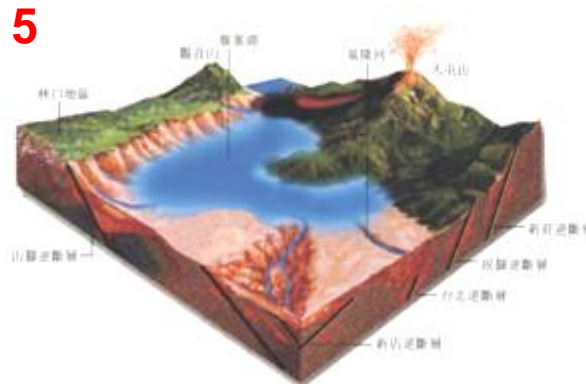
2 Ma
Alluvial fan in Linkou



0.40 Ma
Tectonic extension



0.3 Ma
Conglomerates into
the Taipei basin

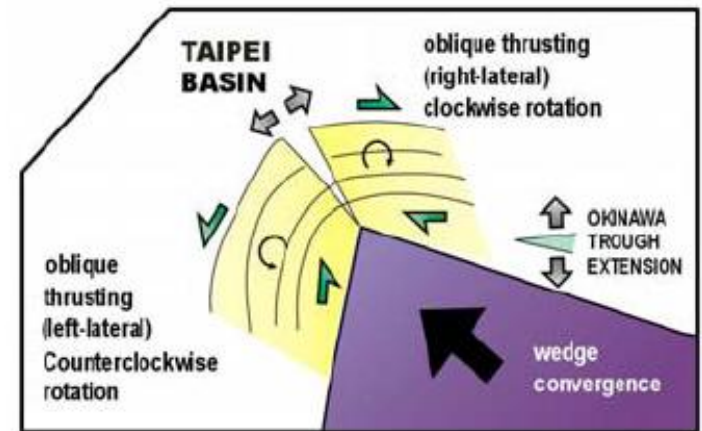
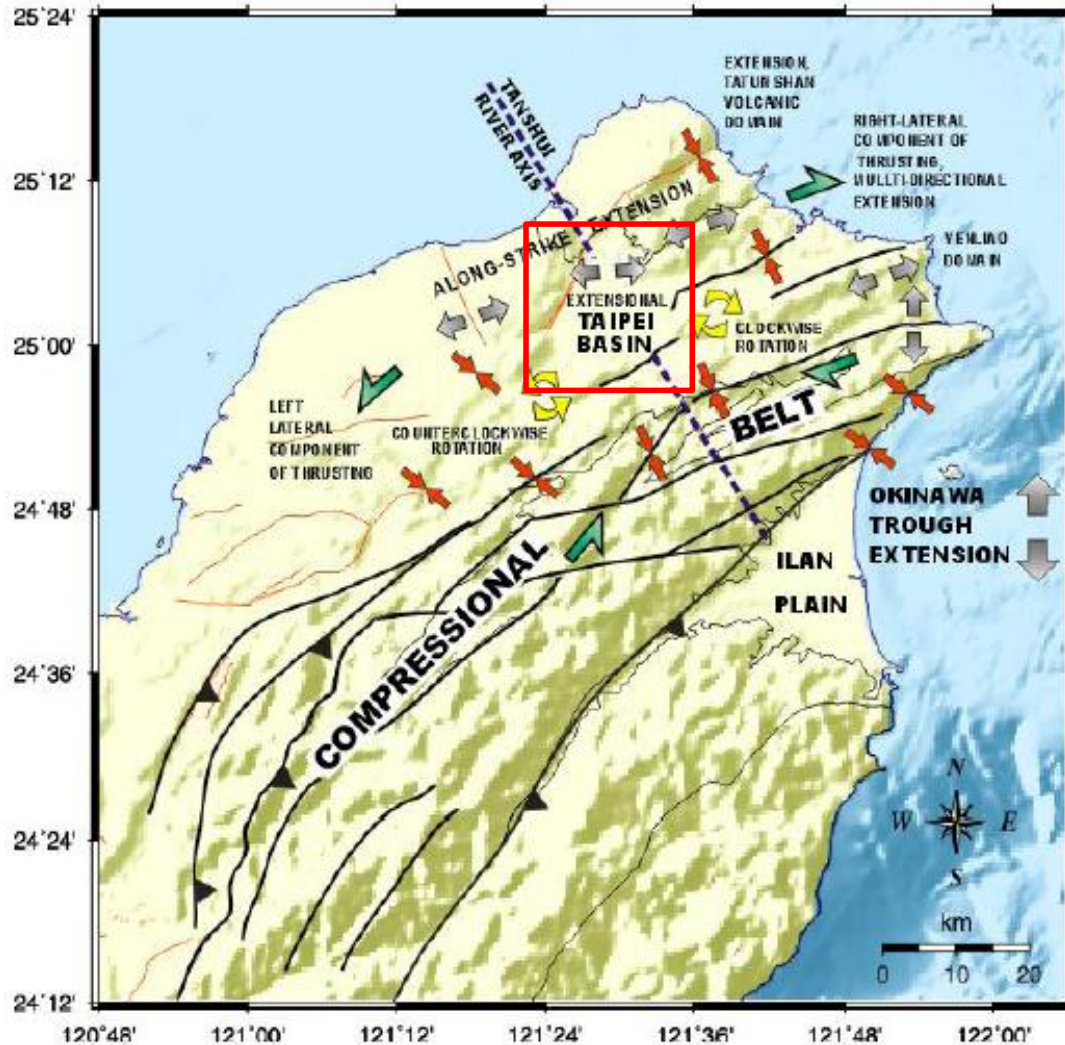


0.2 Ma
Formation of Taipei lake



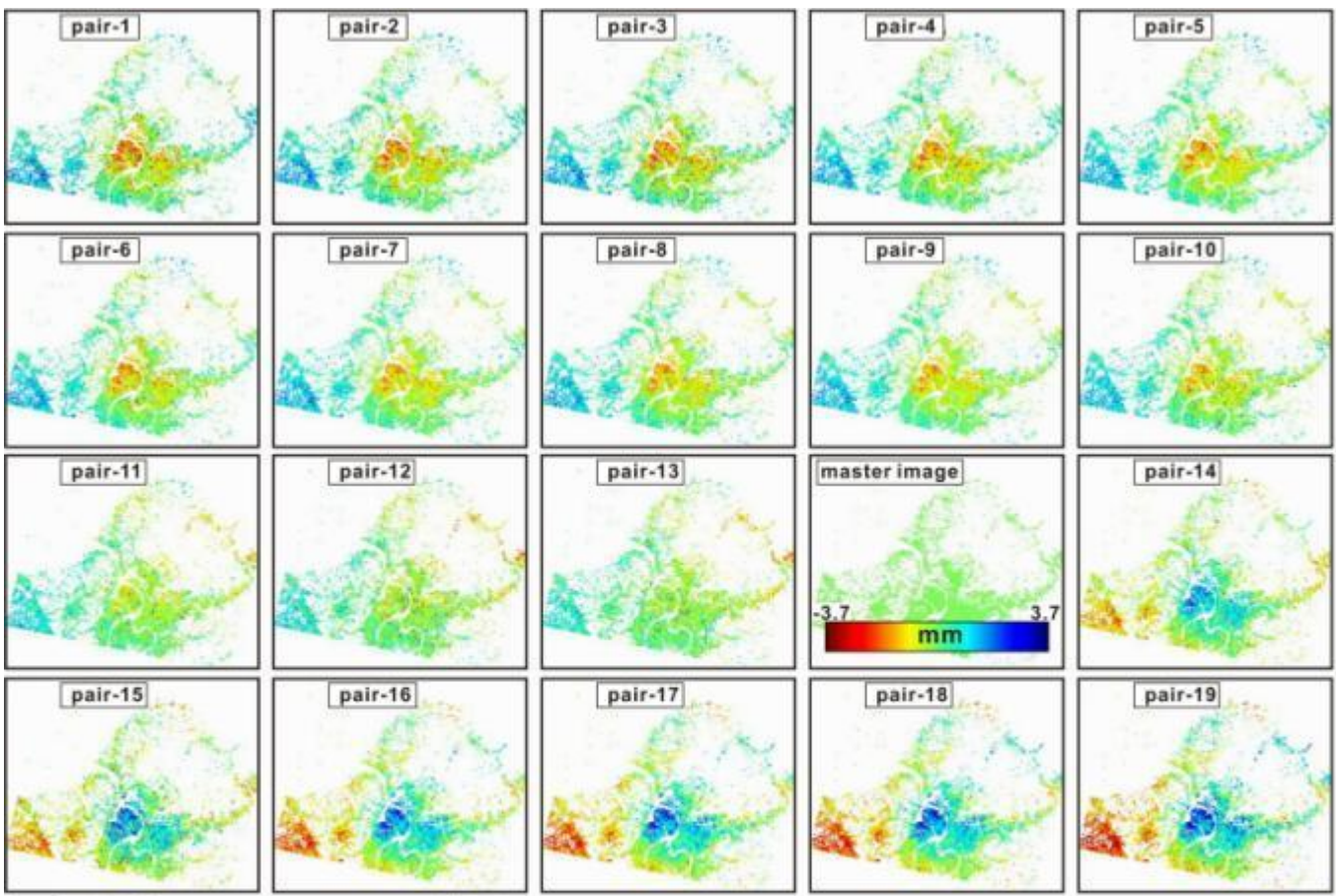
30000 yr ago
River change

Extensional tectonics



Lu *et al.* (1995); Hu *et al.* (2002)

PSInSAR result



Unwrapped phase of PS pixels of each images referenced to the master image.

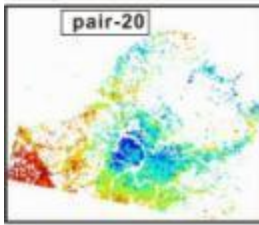
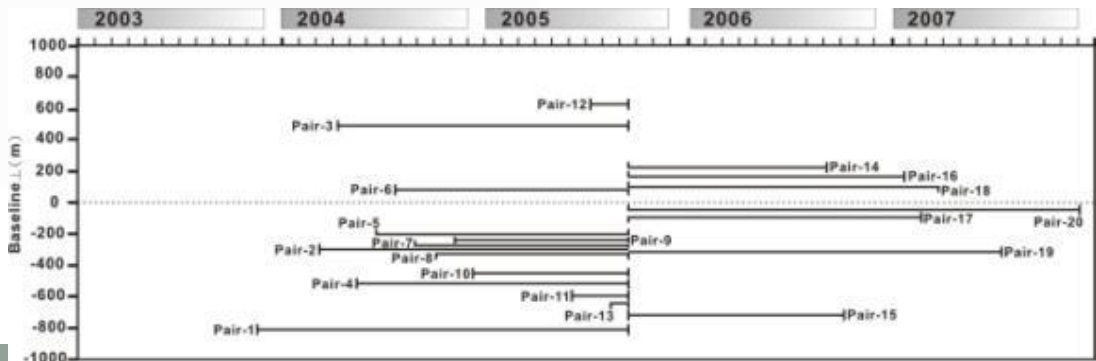
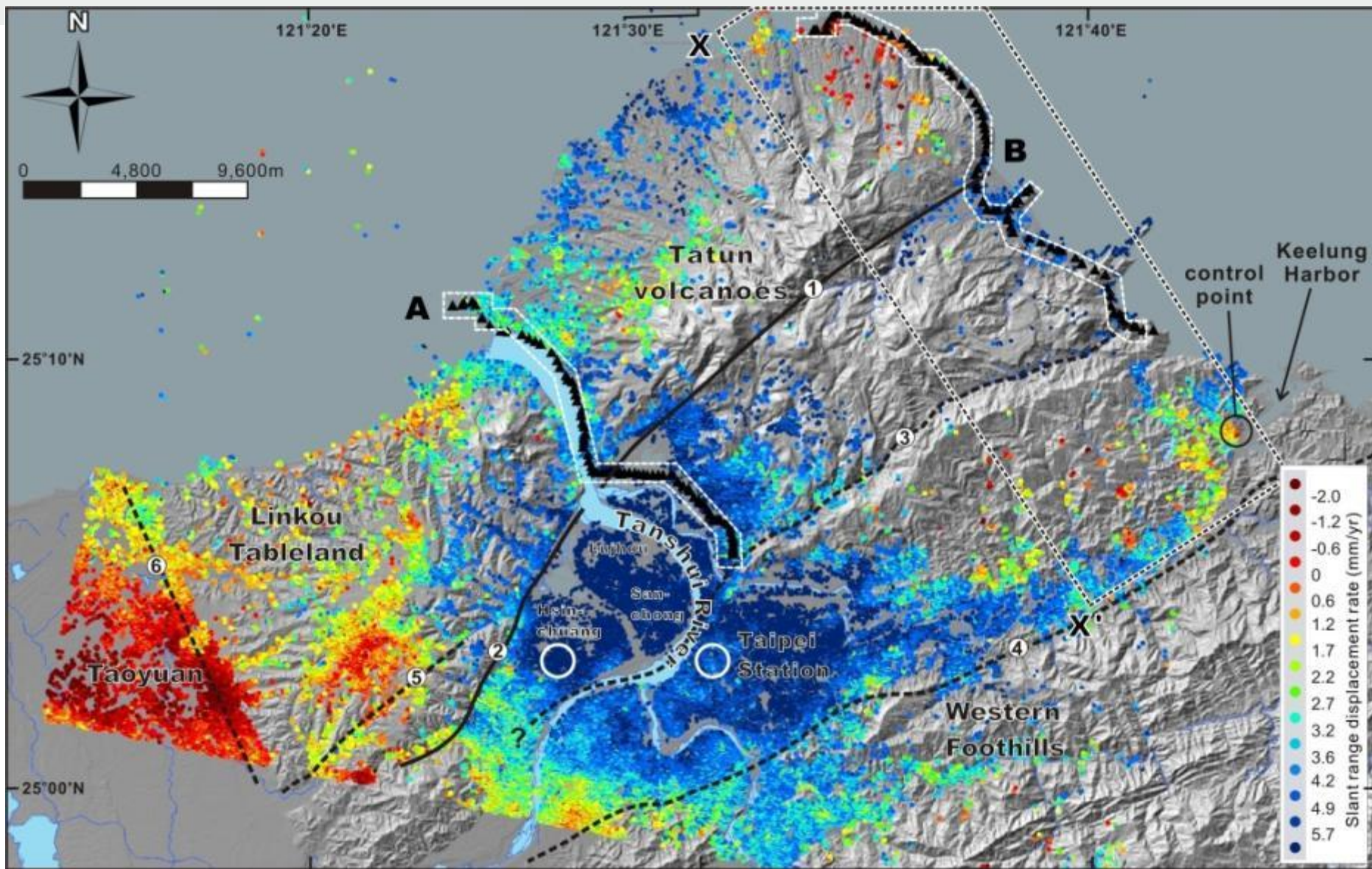


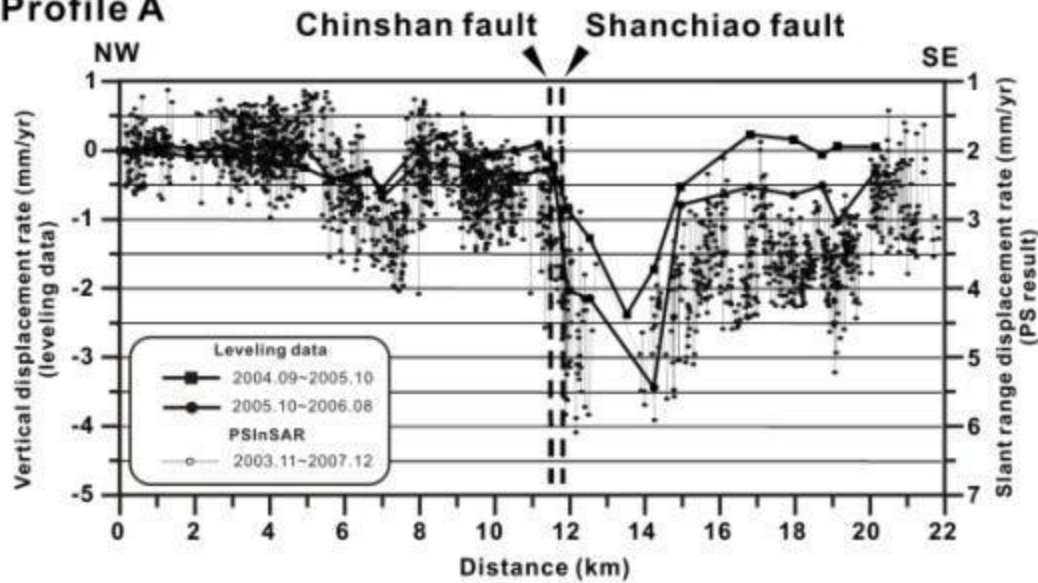
Image pairs used for PSInSAR analysis in this study. All images are acquired by satellite ENVISAT in the descending orbit track 461, frame 3105. The master image is fixed on September 17, 2005.



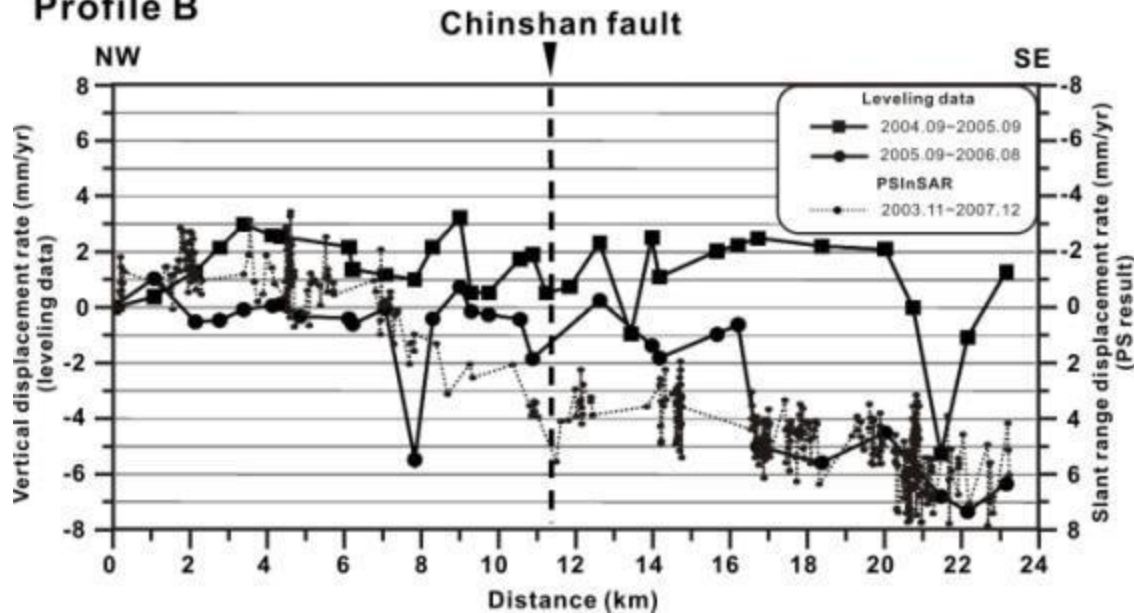


Slant range displacement rate of the processed PSs in the northern Taiwan area. This result has been adjusted by using the base point of “Taiwan Vertical Datum 2001” installed by Ministry of the Interior Bureau in Keelung harbor as the control point. Black triangular: leveling survey points after Hou (2007). White dashed lines encircled the PS pixels that will compare with leveling data along profiles A and B.

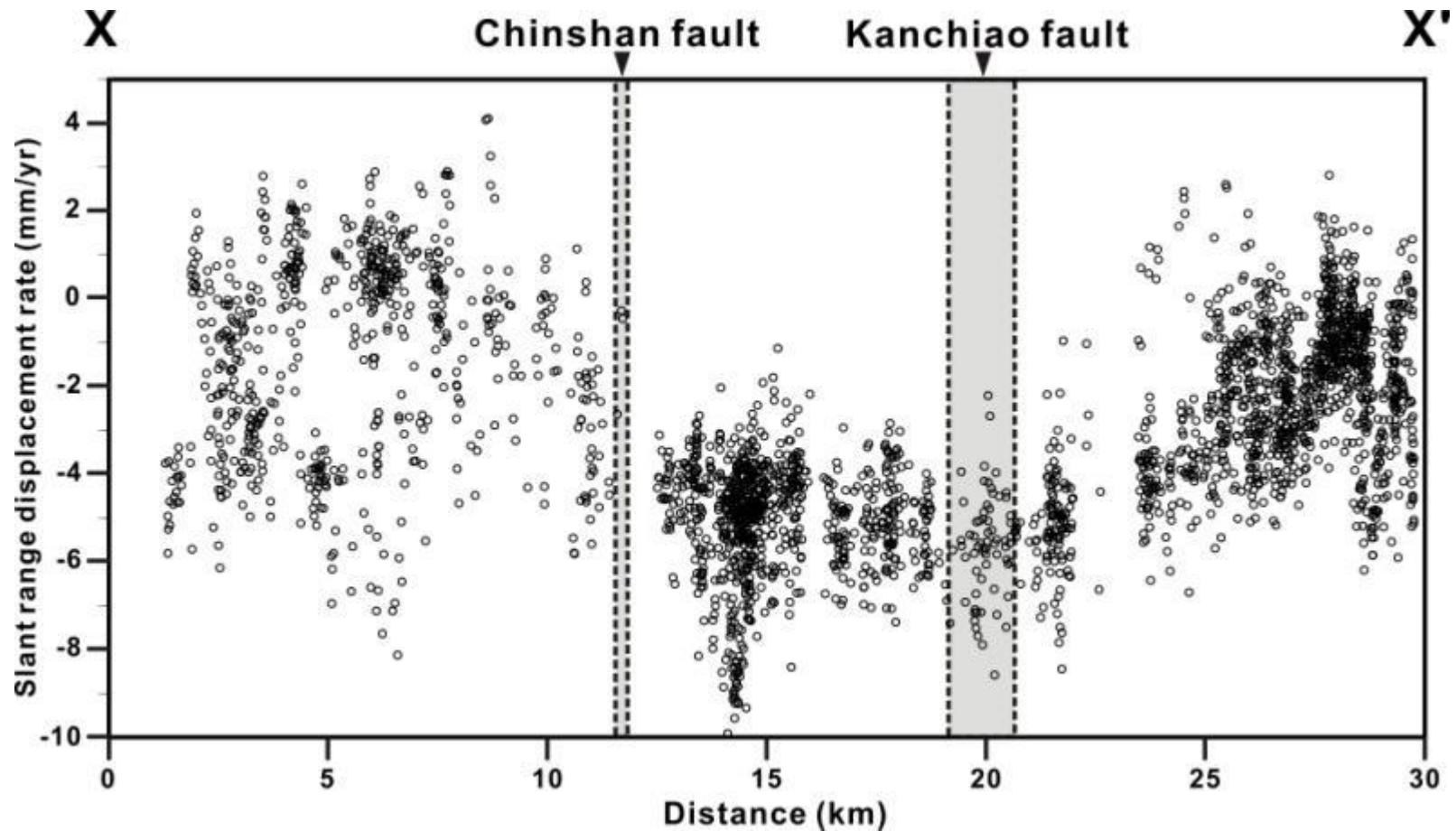
Profile A



Profile B

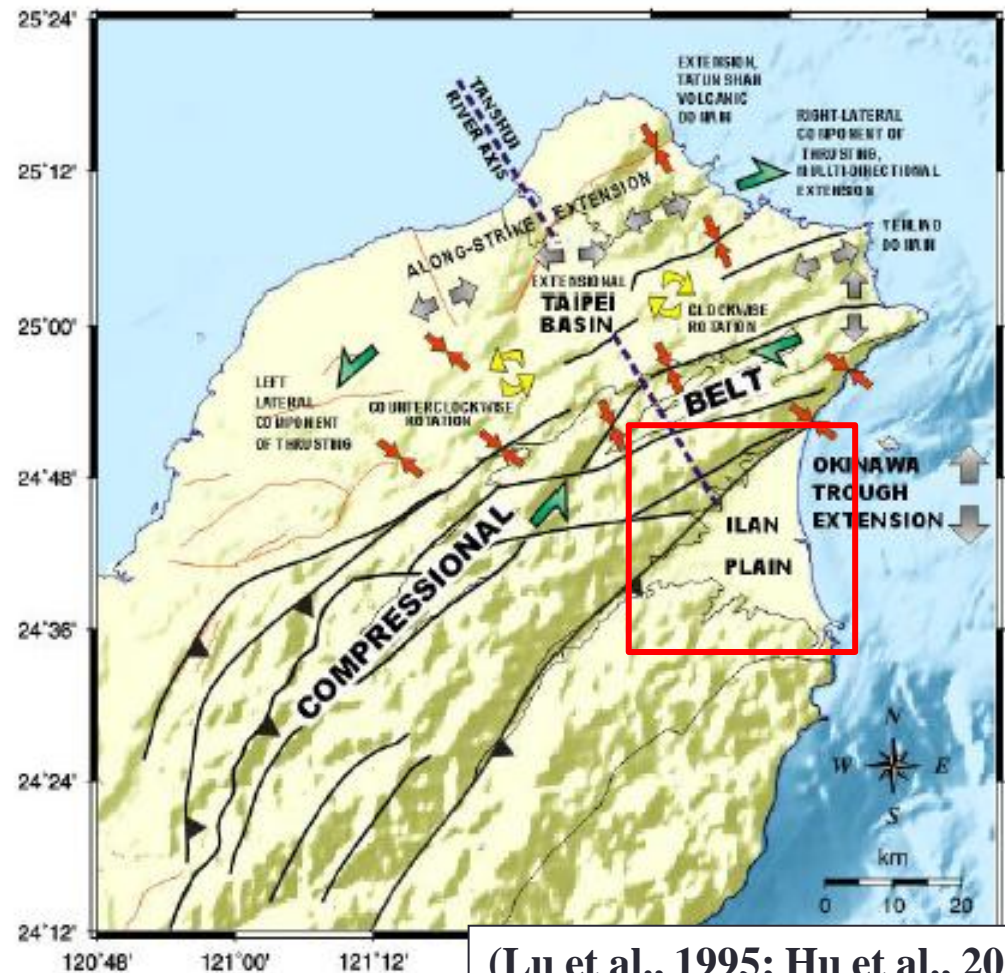


Comparison between the leveling data (Hou, 2007) and PSInSAR result along the northern coastal line (a) and the northern bank of Tanshui River (b). Leveling data are relative to the western most point of the profile, PS displacements are relative to the control point shown in the former figure.



Slant range displacement of PS pixels in the northern tip of Taiwan Island (in frame XX'). Clear subsidence can be observed in the terrain between the Chinshan and Kanchiao Faults.

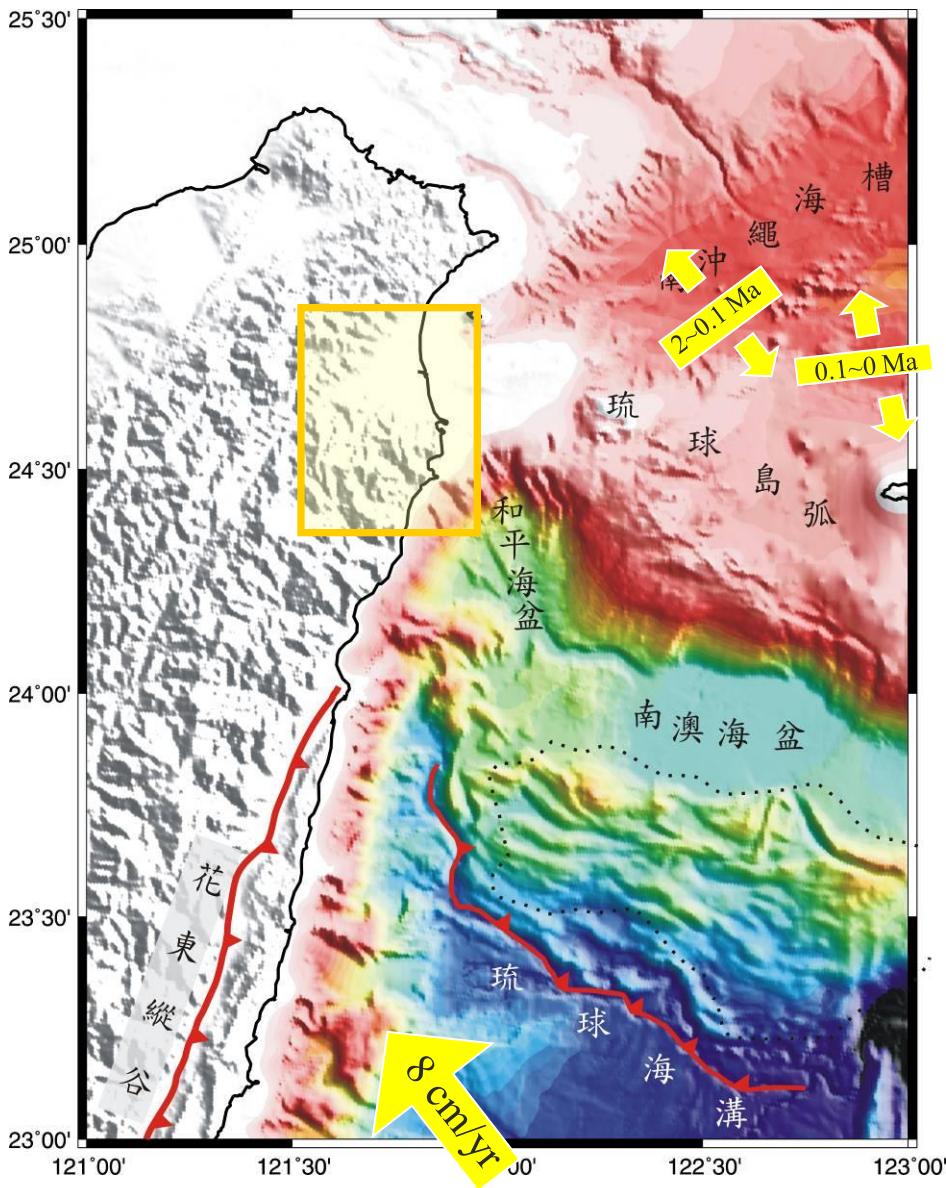
ILan plain



(Lu et al., 1995; Hu et al., 2002)

- 320 Km² in area
- Triangular alluvial plain
- Southern tip of the Okinawa Trough

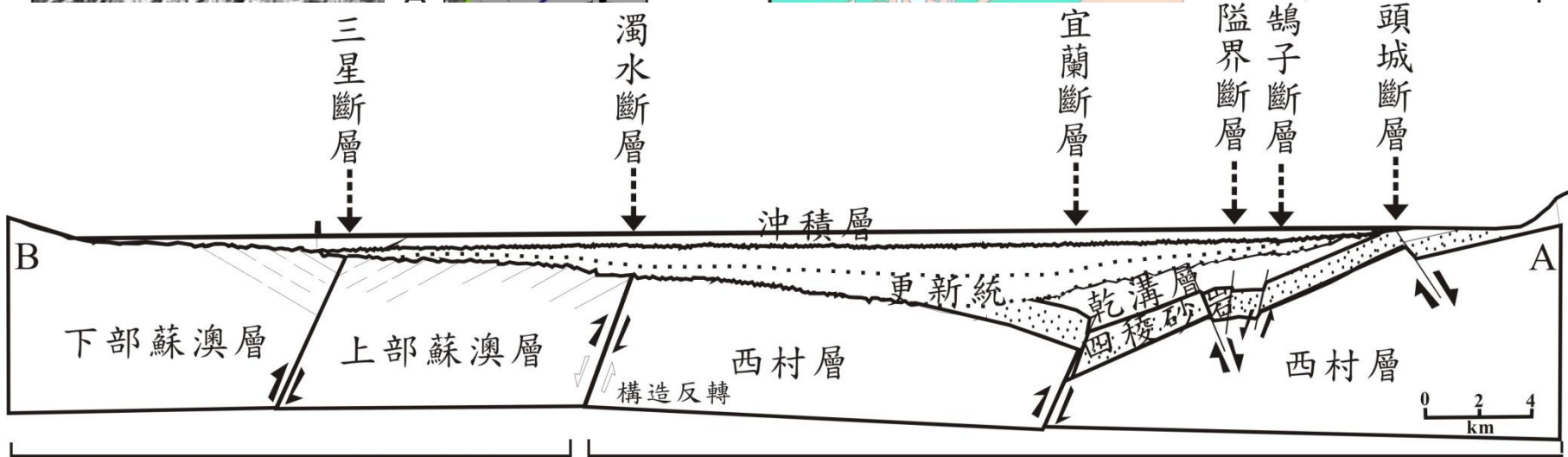
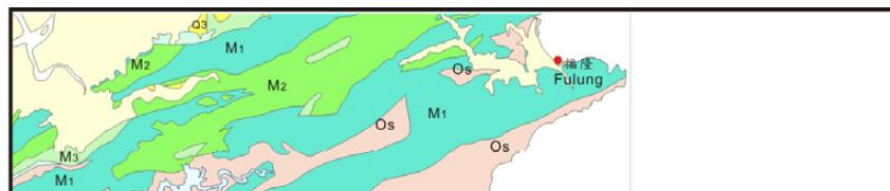
background



蘭陽平原地區東側之地體構造：

- 1、南沖繩海槽的張裂
- 2、琉球海溝之隱沒系統
- 3、菲律賓海板塊斜向擠壓

Geological setting of the Ilan Plain



脊梁山脈

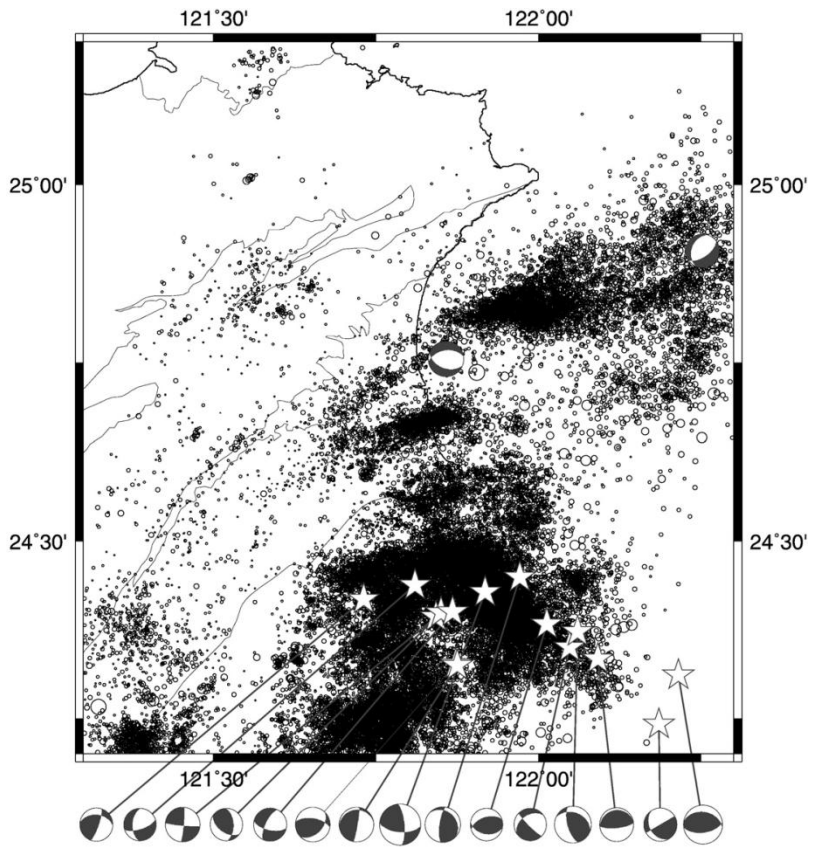
雪山山脈



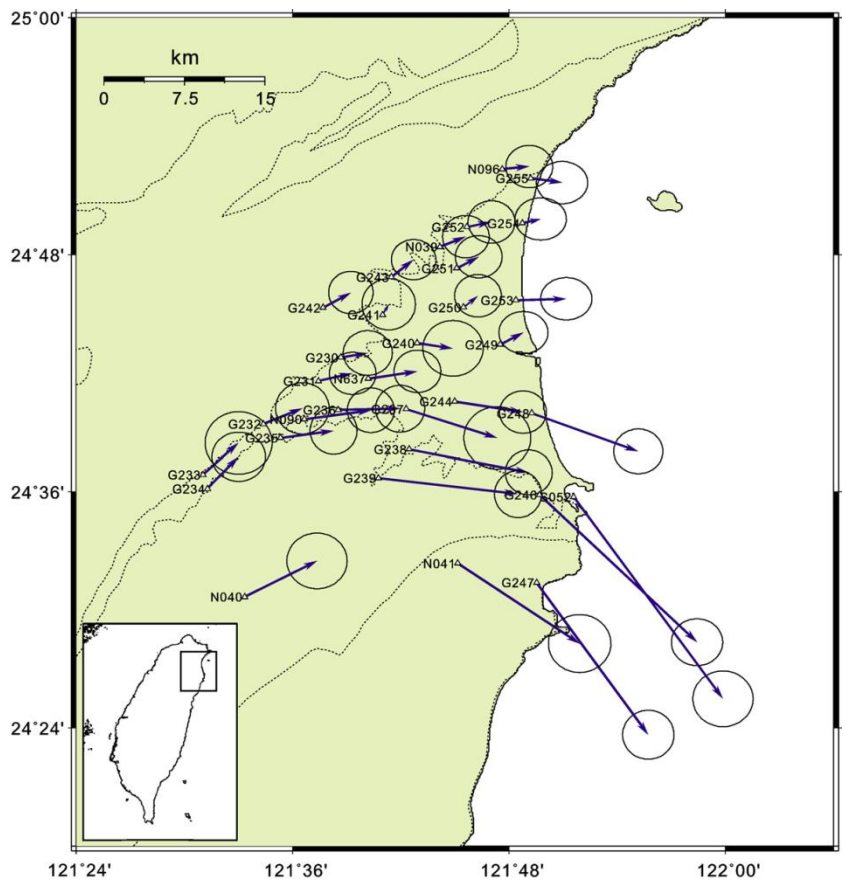
- (Chaing, 1976)
- (Lee et al., 1998)
- (Yu et al., 1979)
- (Shyu et al., 2005)
- (Tsai, 1976)

(中央地調查所五十萬分之一地質圖、江新春, 1976)

Geophysical data



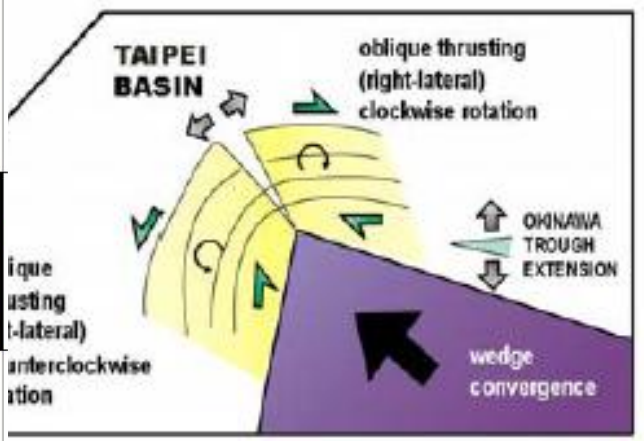
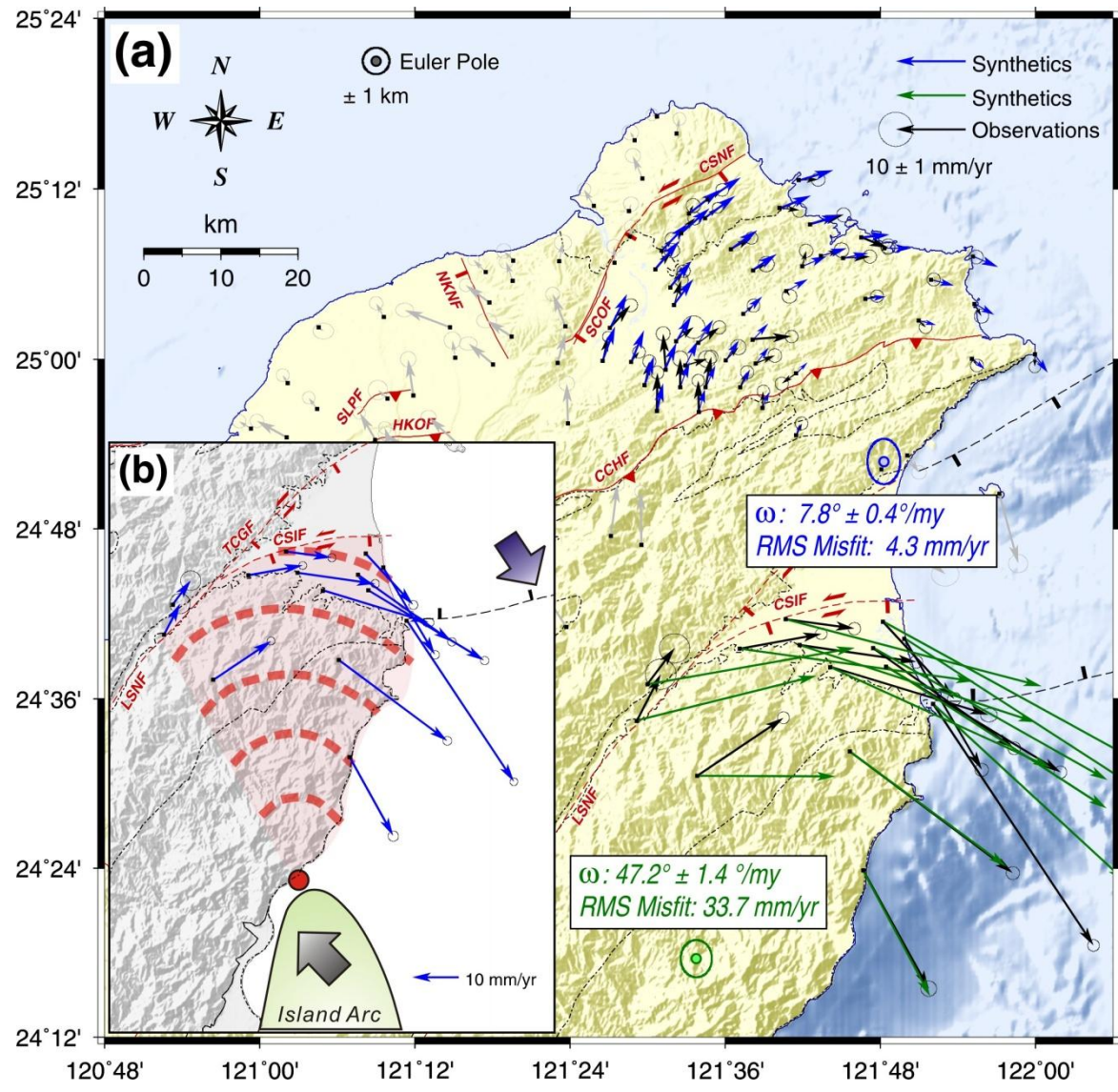
Seismicities of $M_L > 3$ in northeastern Taiwan from 1994 to 2000 based on the Catalog of CWB. The focal mechanisms of magnitude 5.0 to 6.0 are shown.



GPS velocity field

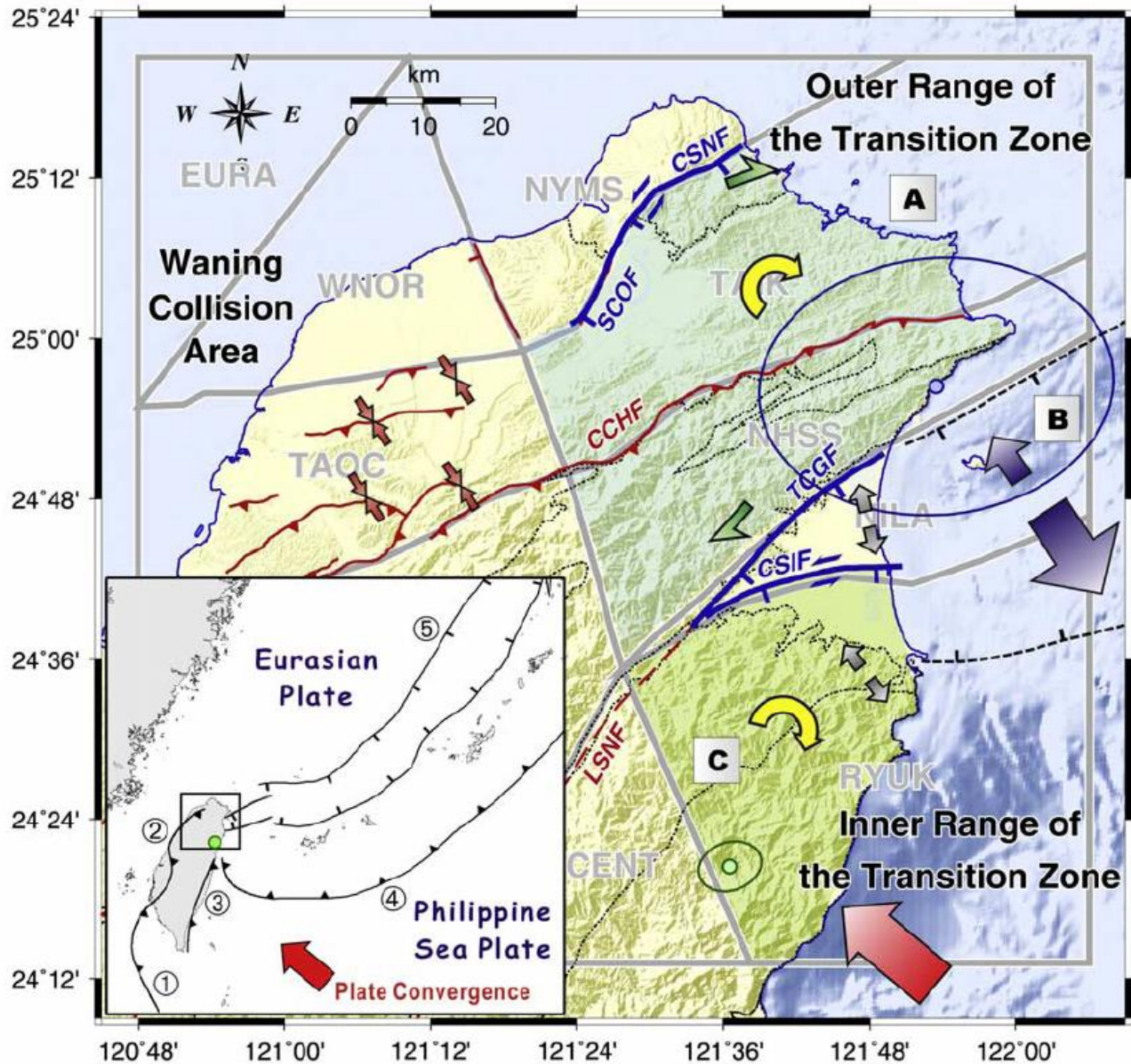
(Hou et al., 2009)

Clockwise rotation

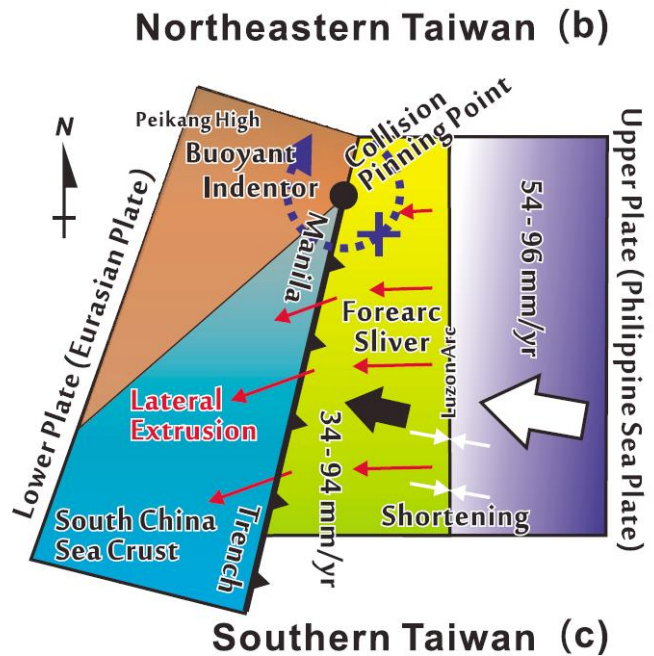
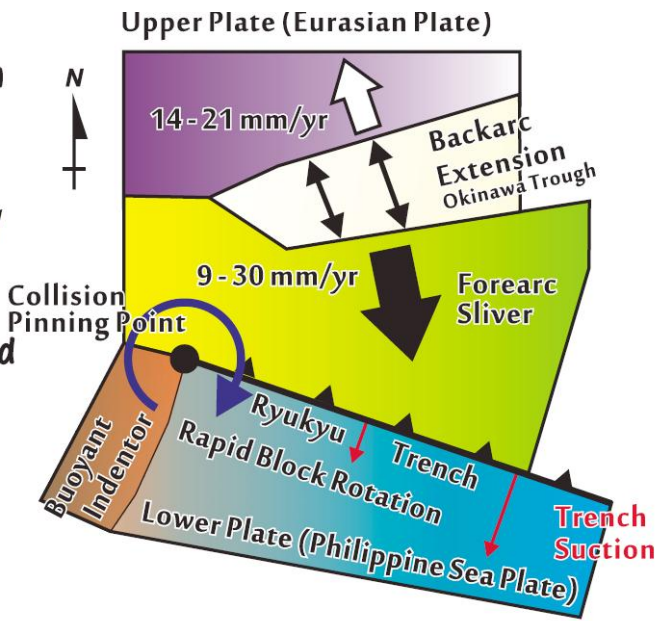
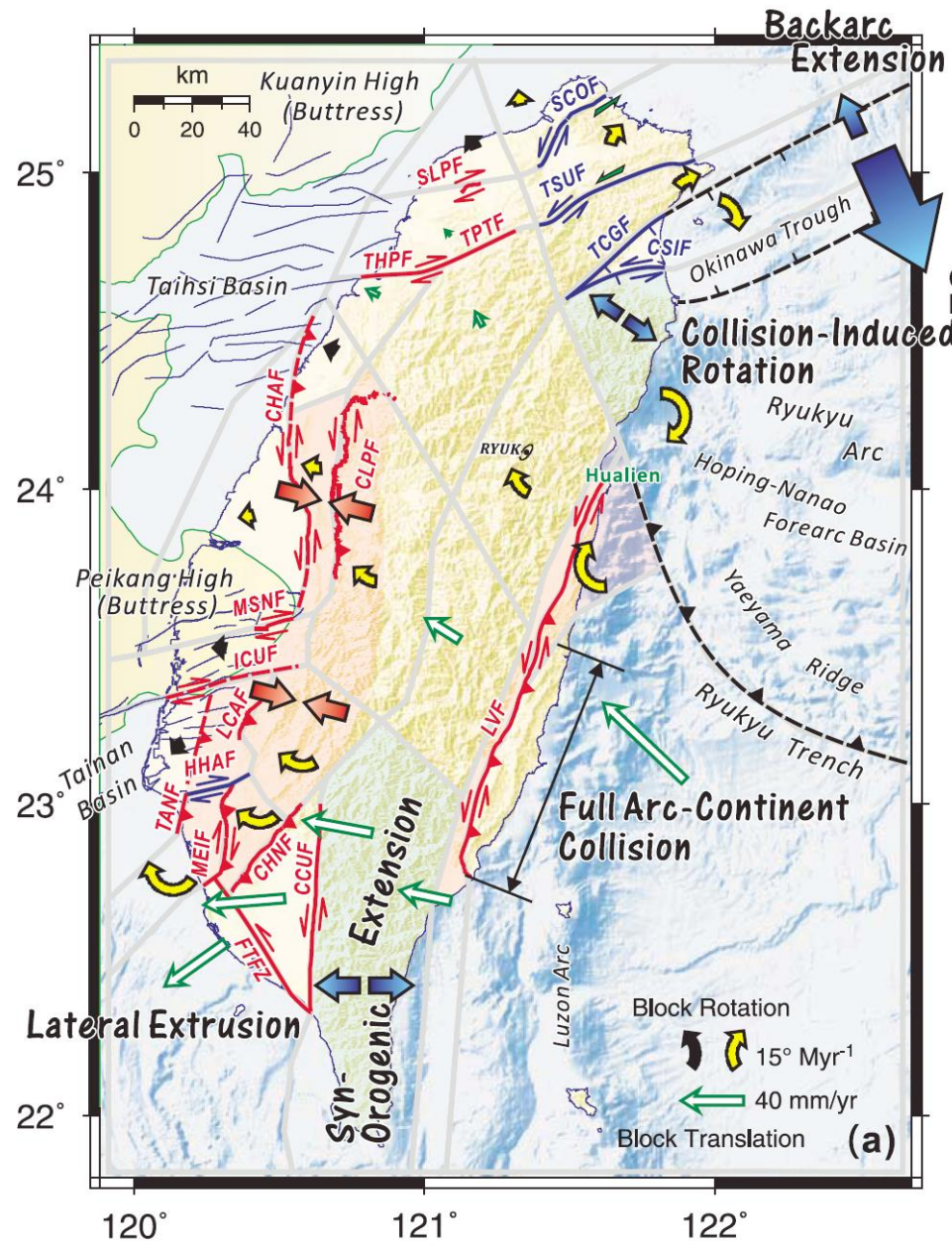


Lu *et al.* (1995); Hu *et al.* (2002)

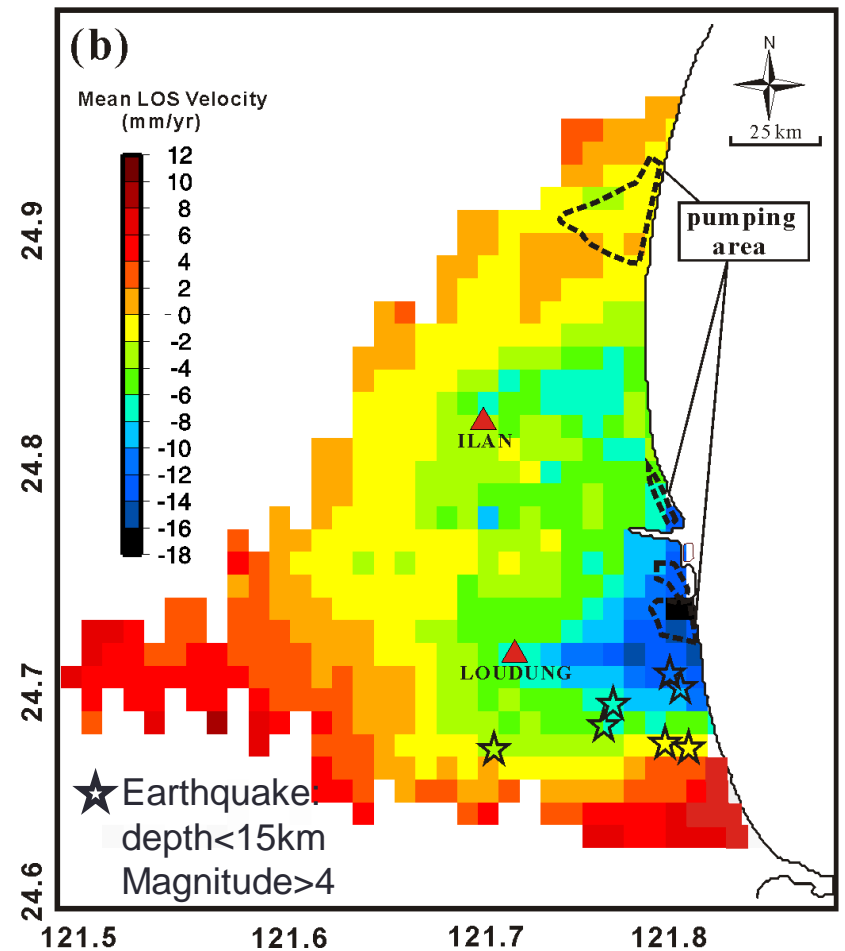
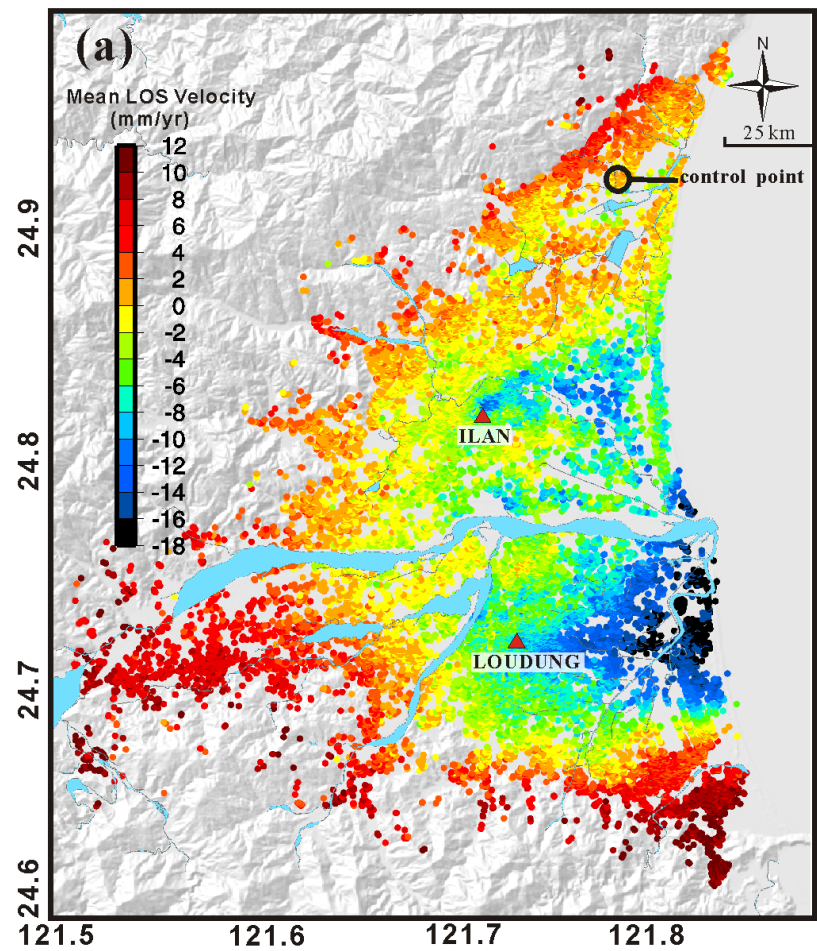
The tectonic model



Schematic of the strain-partitioning model

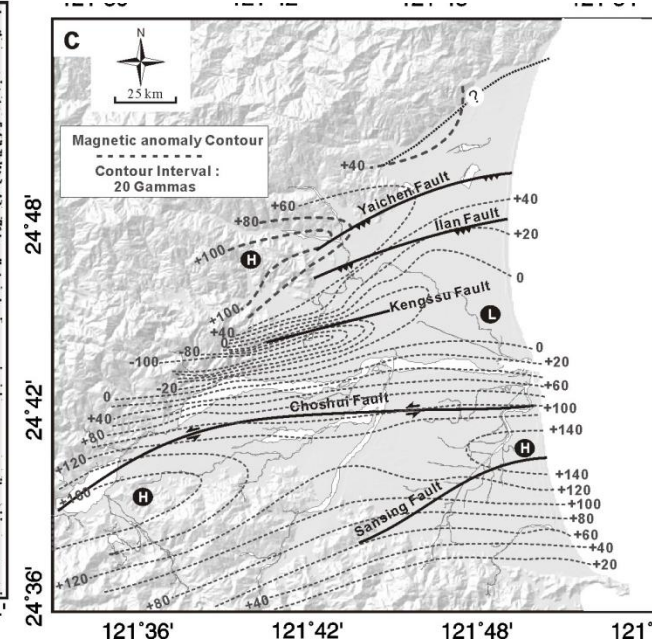
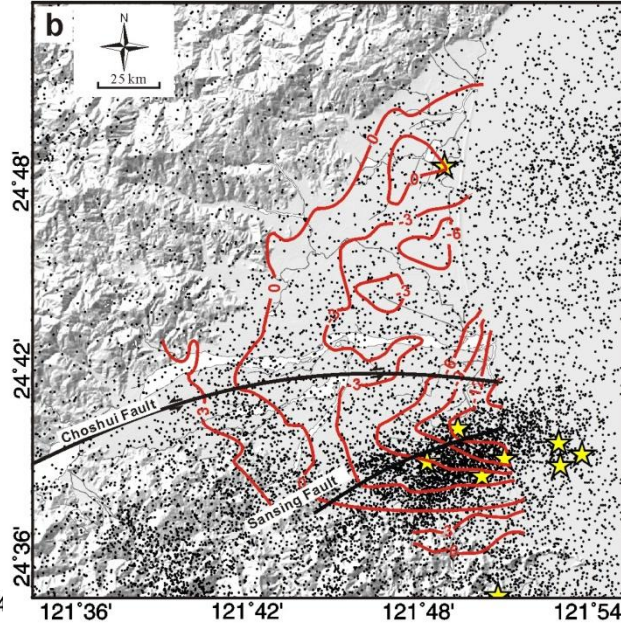
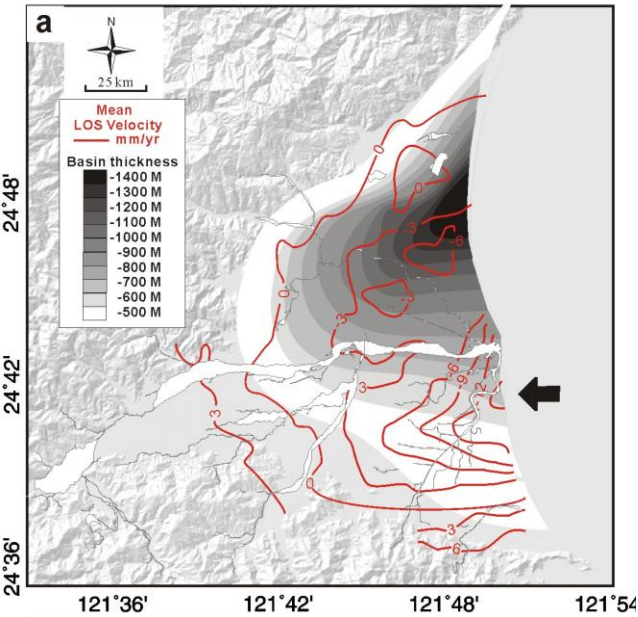


PSInSAR result



(a) Mean LOS velocity of the processed PS and mound in the Ilan Plain.
(b) Interpolated LOS velocity of the PSI results.

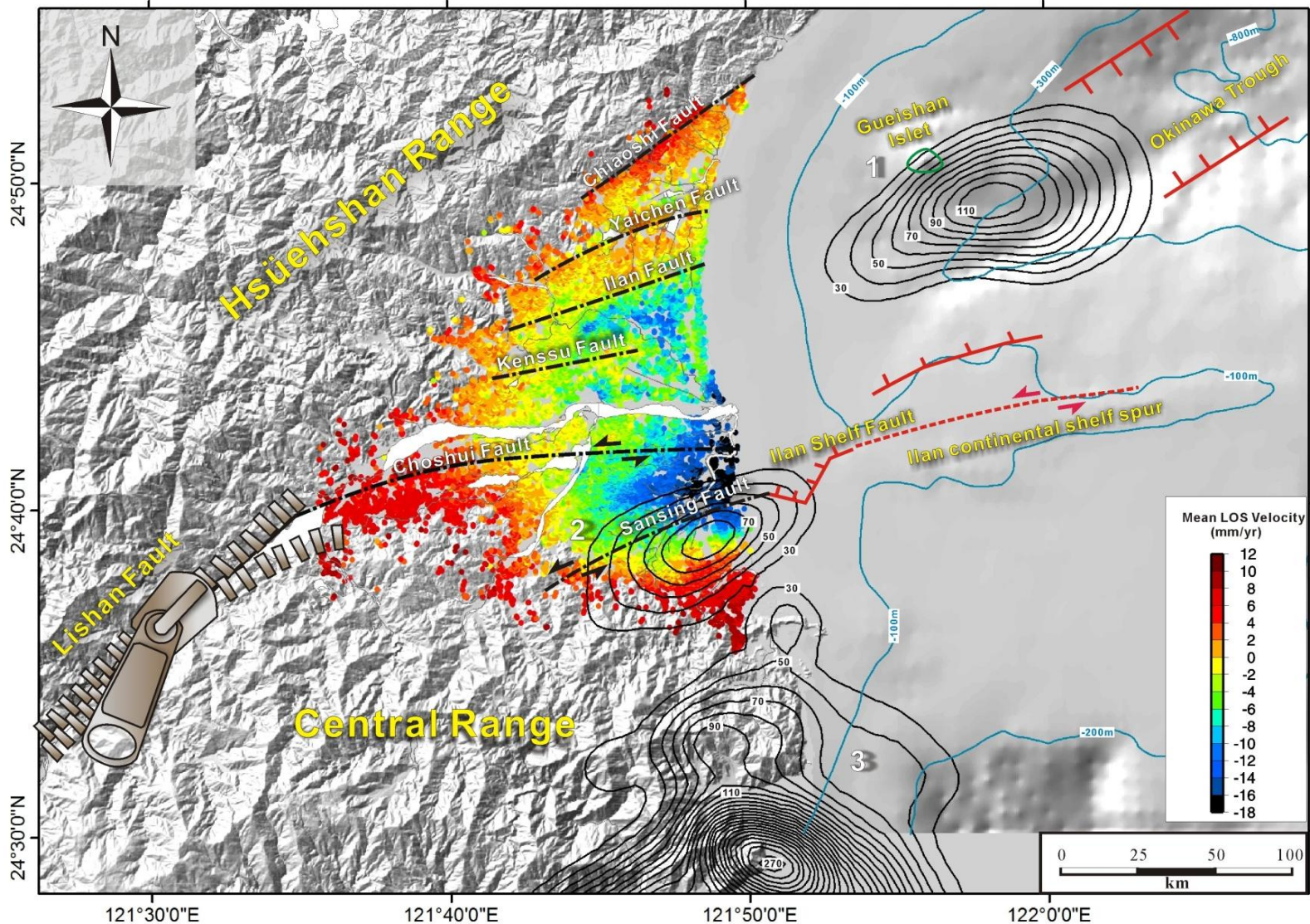
Relationships between surface deformation and basement structures



a) Map of the Plio-Quaternary basin thickness in the Ilan Plain (after Jhiang, 1976). Red solid lines show the PSI mean LOS velocity contours and the black arrow highlights the area with the highest subsidence rate.

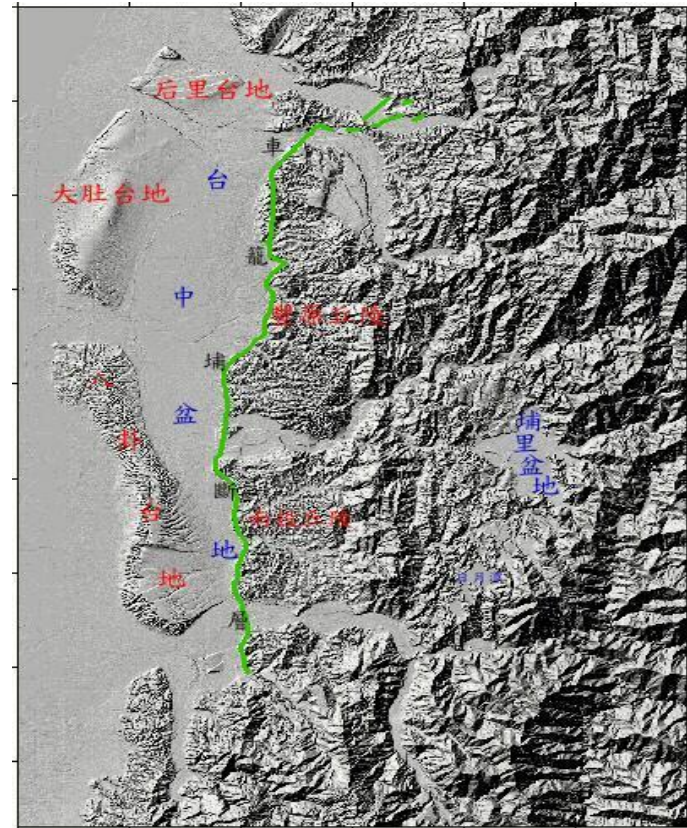
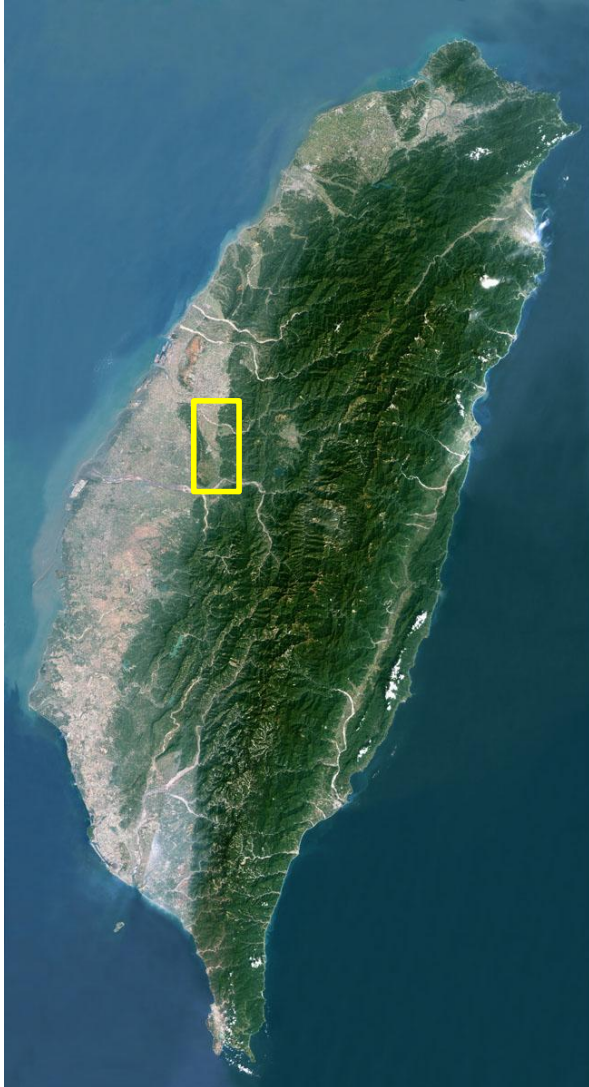
b) Seismicity distribution map from 1994 to 2008 (Central Weather Bureau Earthquake Catalogue). Yellow stars locate earthquakes with $M_L > 3$ and depth lower than 30 km. Red solid lines show the PSI mean velocity contour.

c) Contour map of the magnetic anomalies in the Ilan Plain (after, Yu and Tsai, 1979).



The zipper-like mode for the propagation of the Okinawa Trough through the Taiwan mountain belt, reactivating basement faults that were originally back-thrusting the Hsüehshan Range onto the Central Range (Lishan-Choshui faults).

Taichung basin

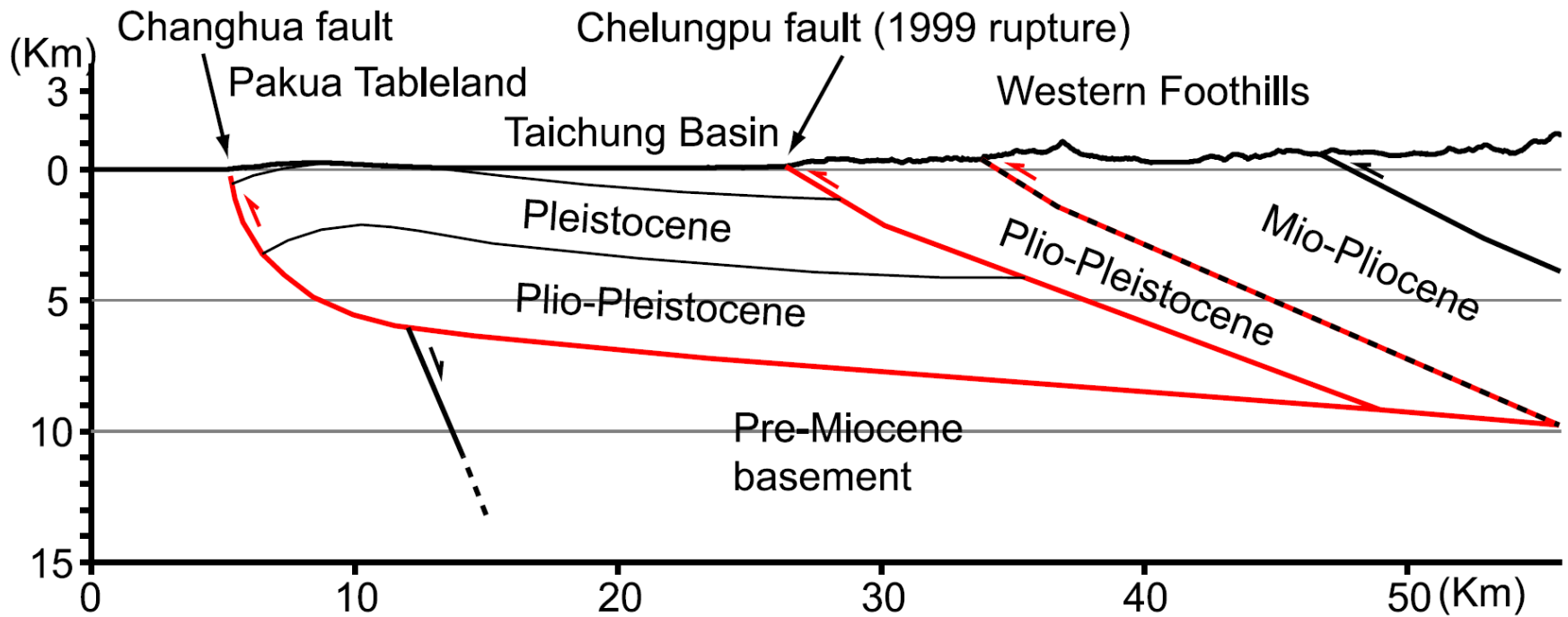


- 370 Km² in area
- Elongated in shape
- Between two thrusts

Geotectonic setting



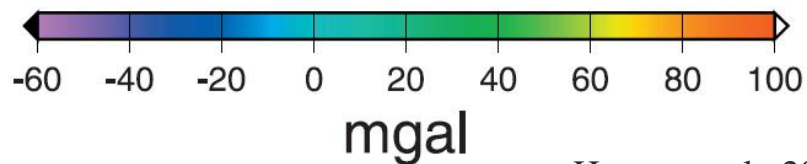
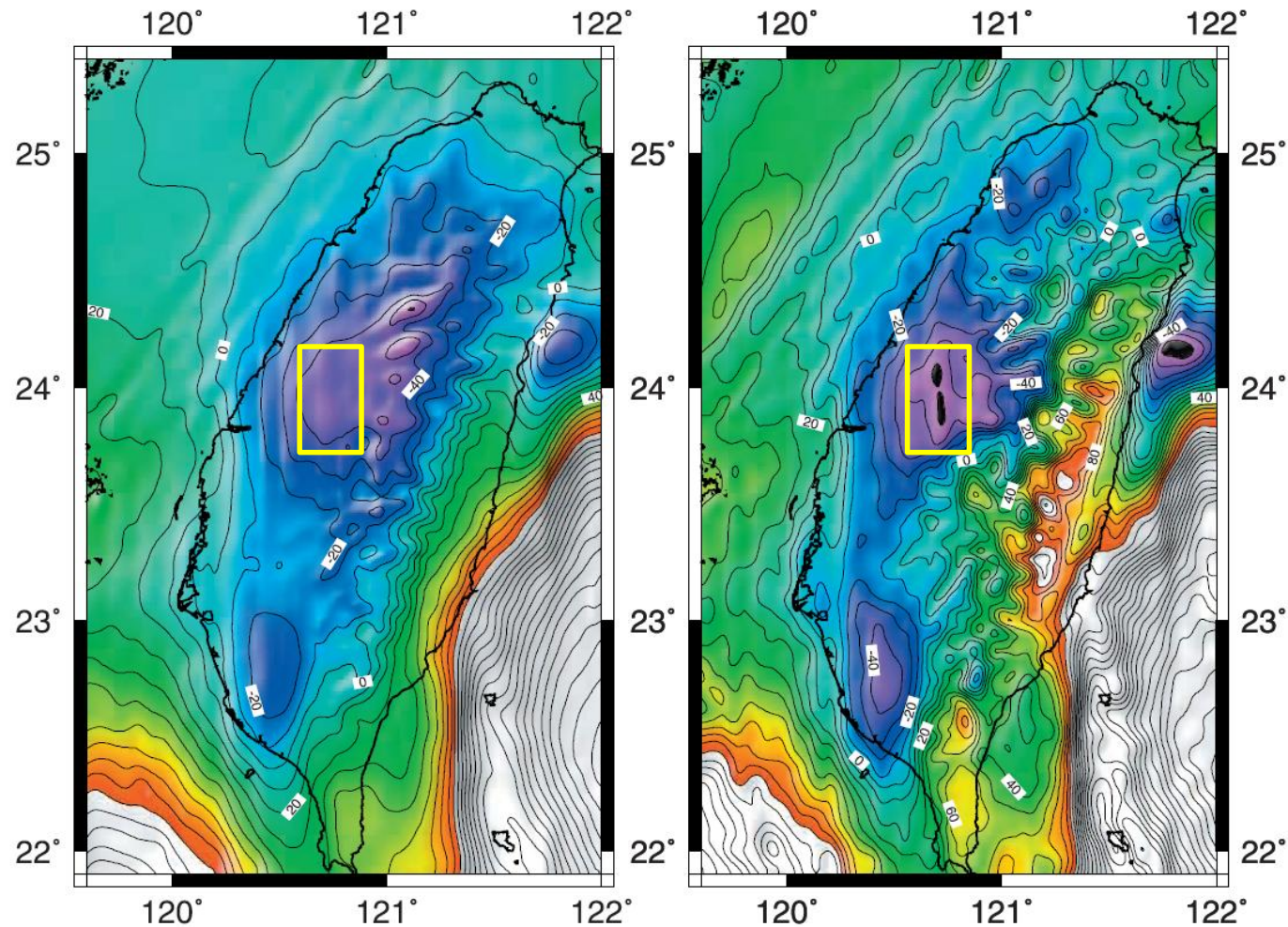
(g) Taichung Domain



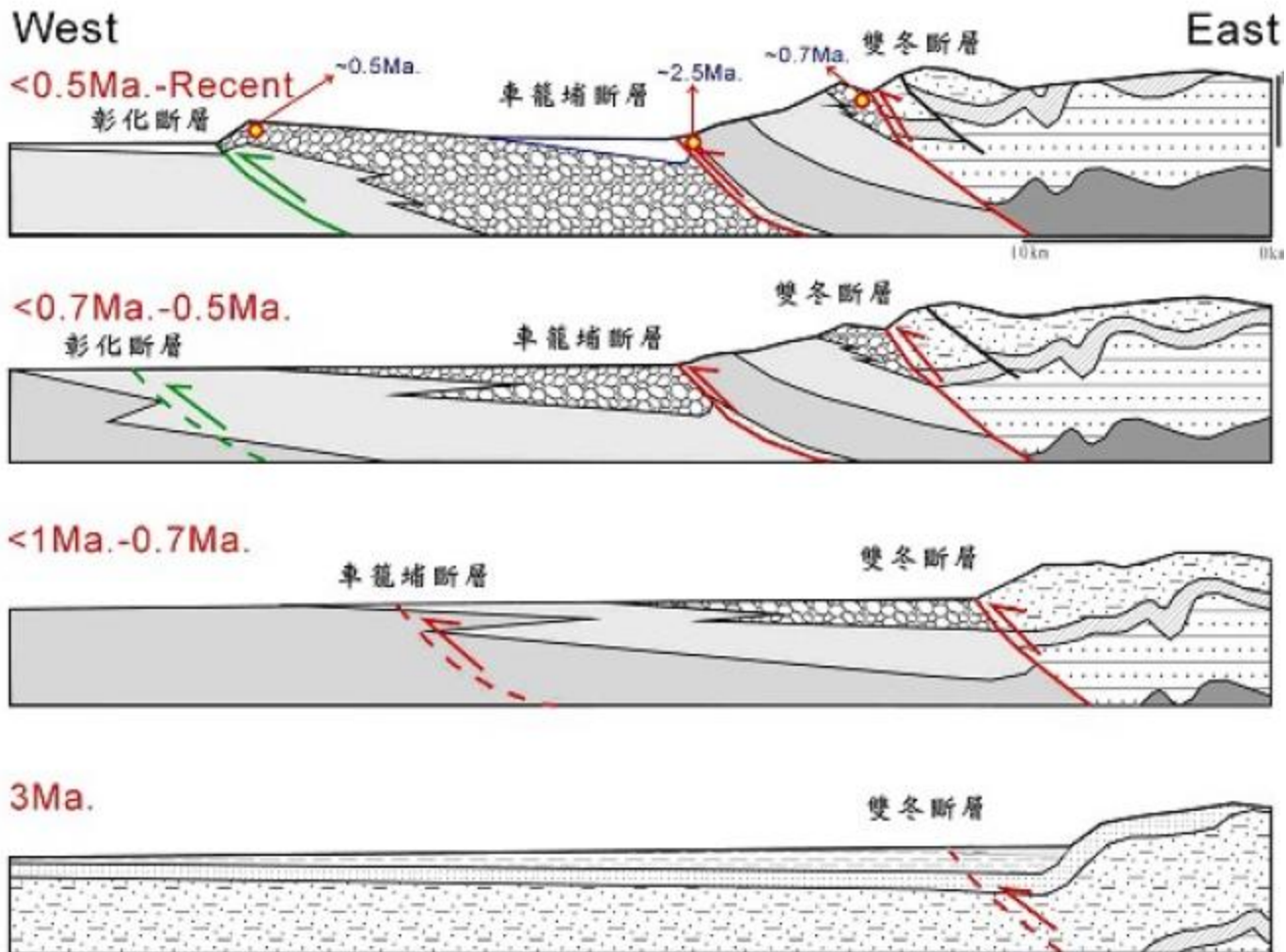
The Bouguer anomalies

At the flight altitude

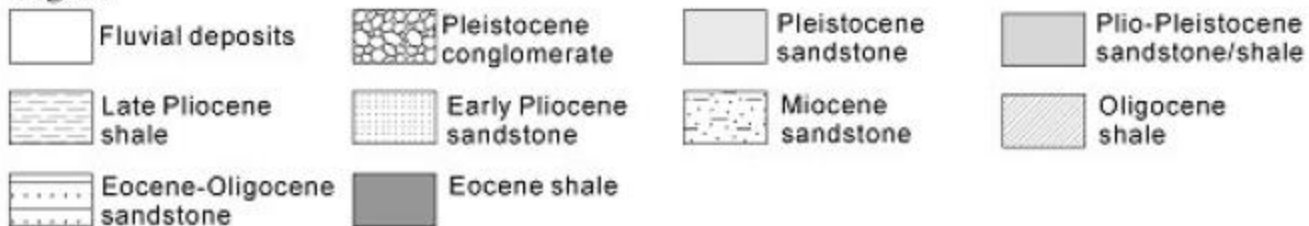
At sea level



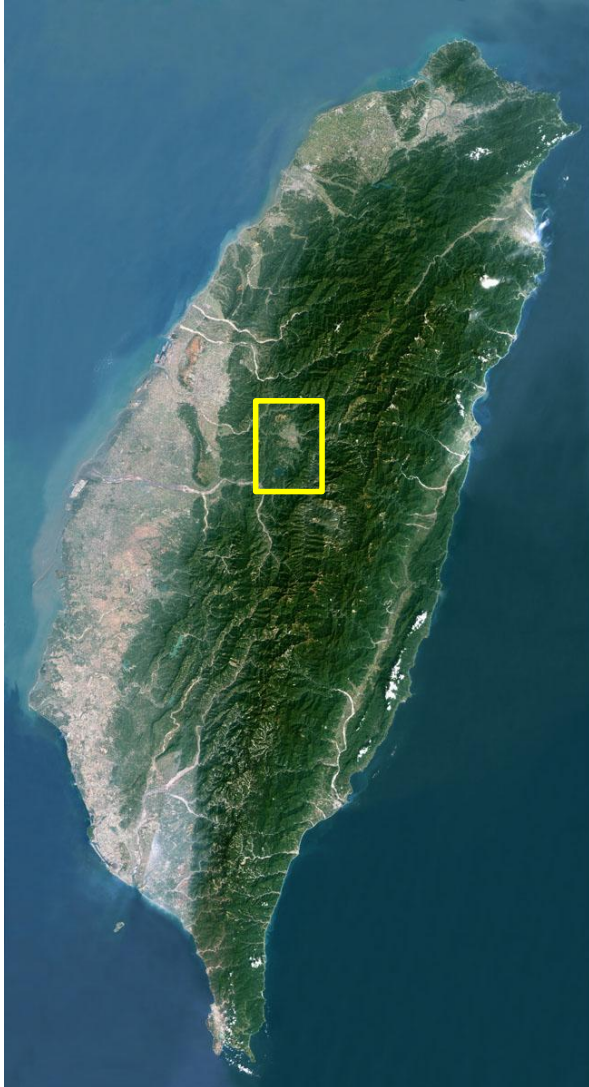
台中盆地的重力低區
➤ 近地表厚層的沉積層所造成，且有一滑脫面位於深部。



Legend



Puli basin

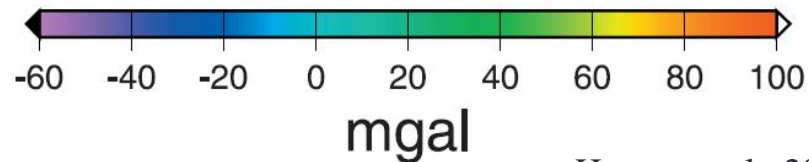
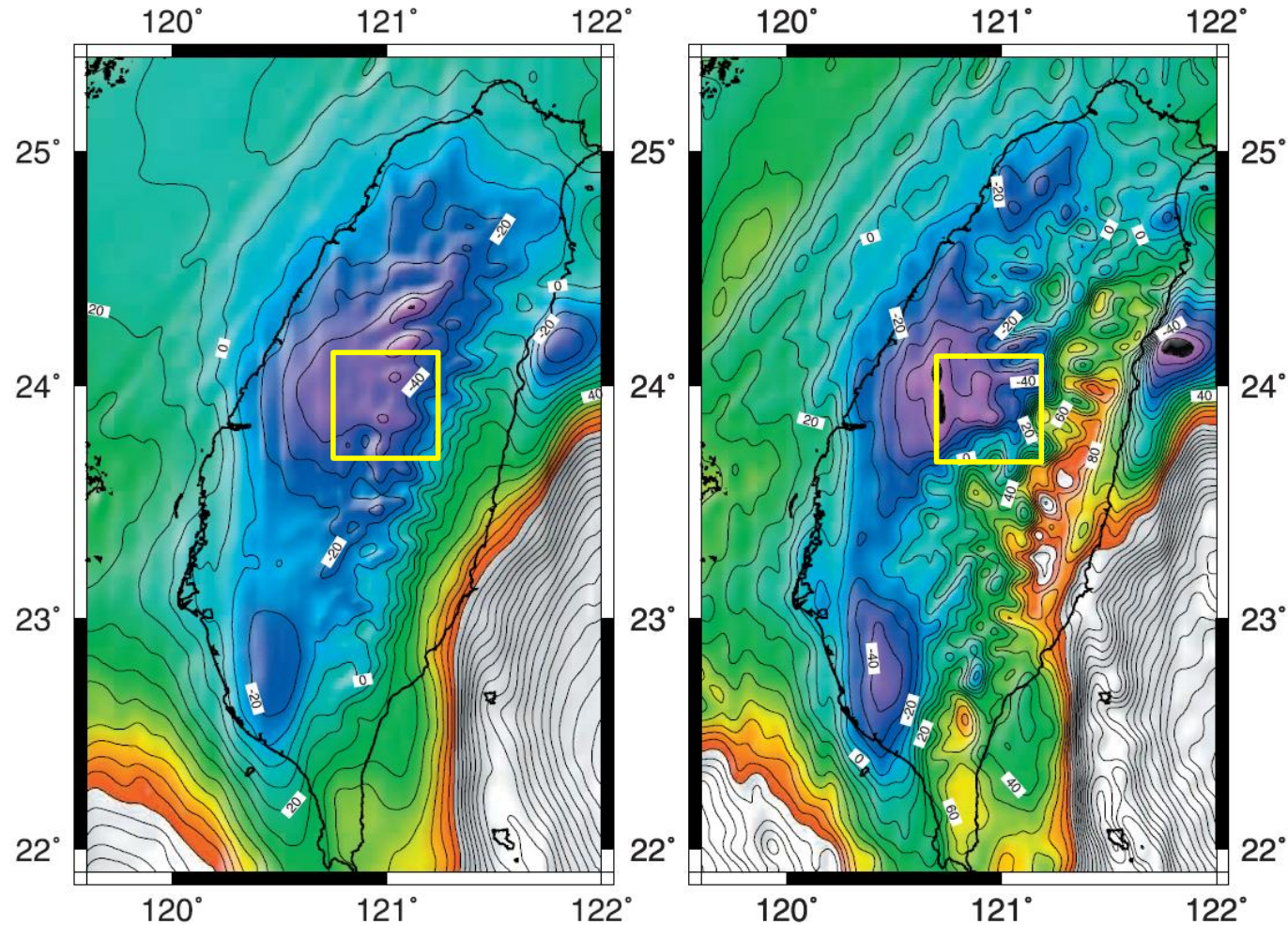


- 42 km² in area
- Gravity Low
- A series of basins
- Intra-Mountain basin

The Bouguer anomalies

At the flight altitude

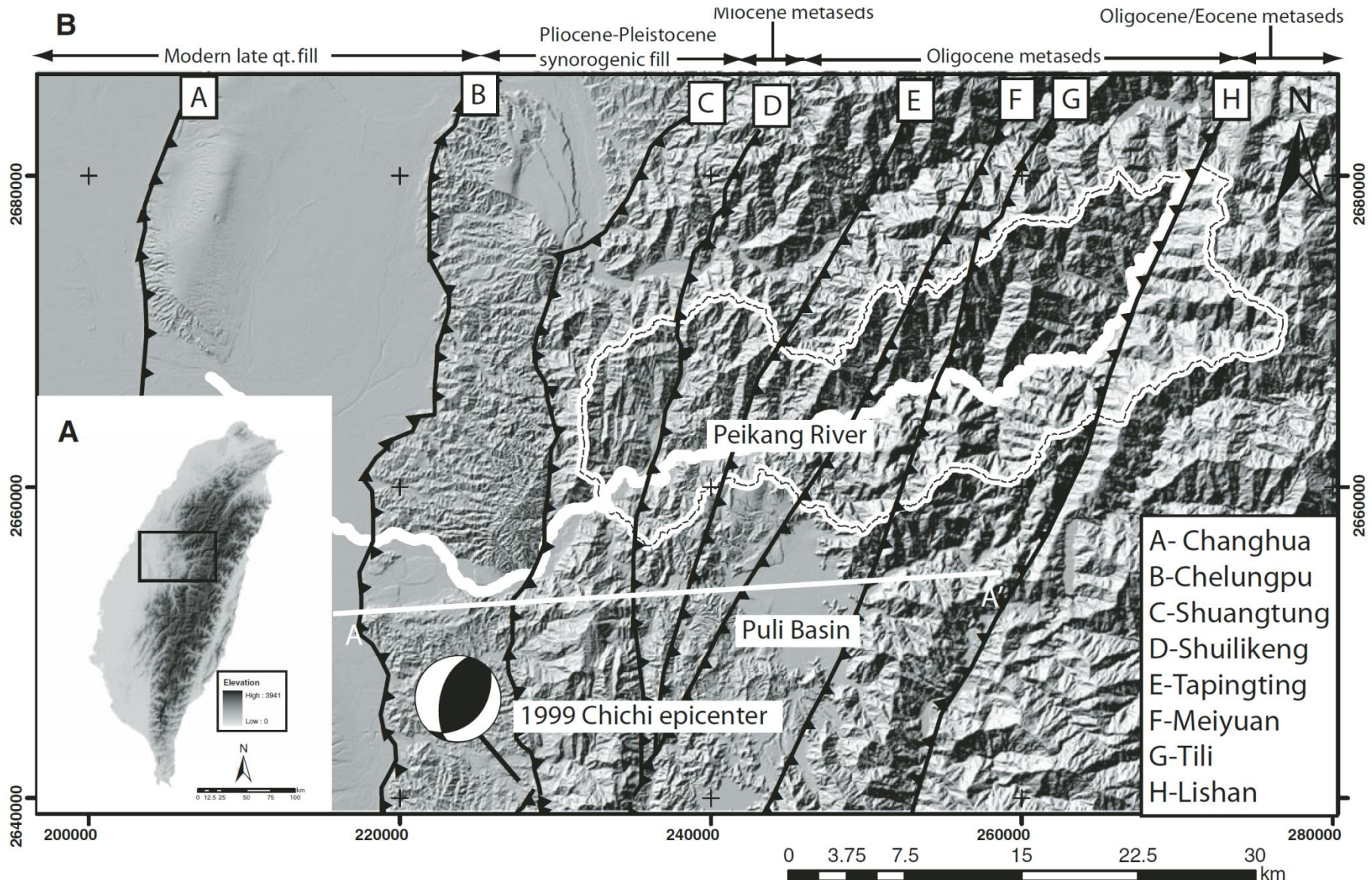
At sea level



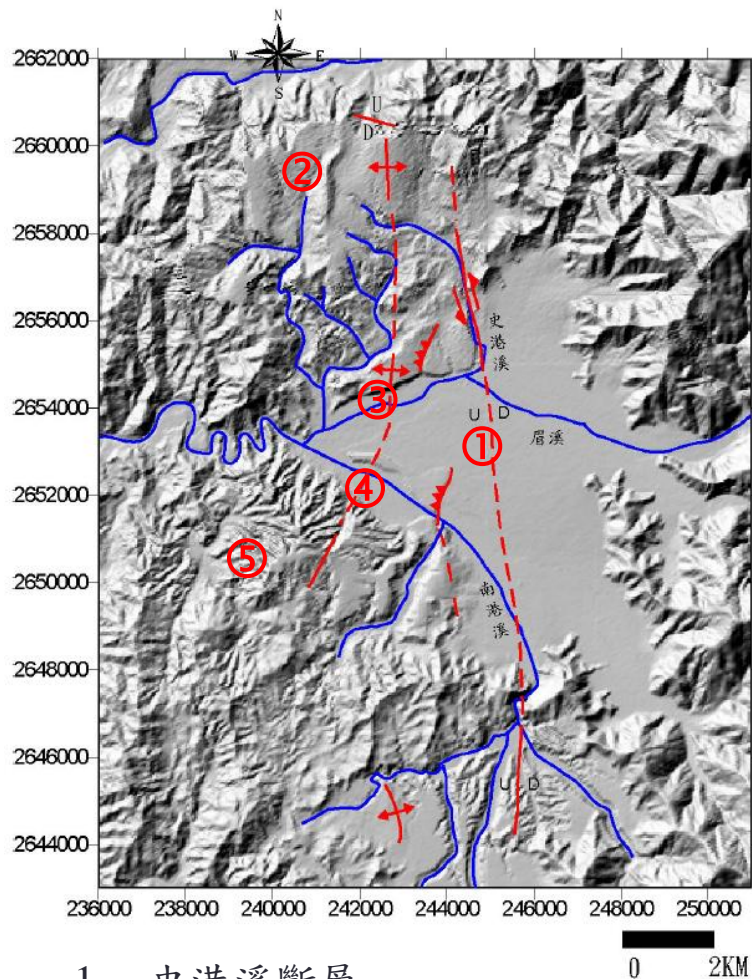
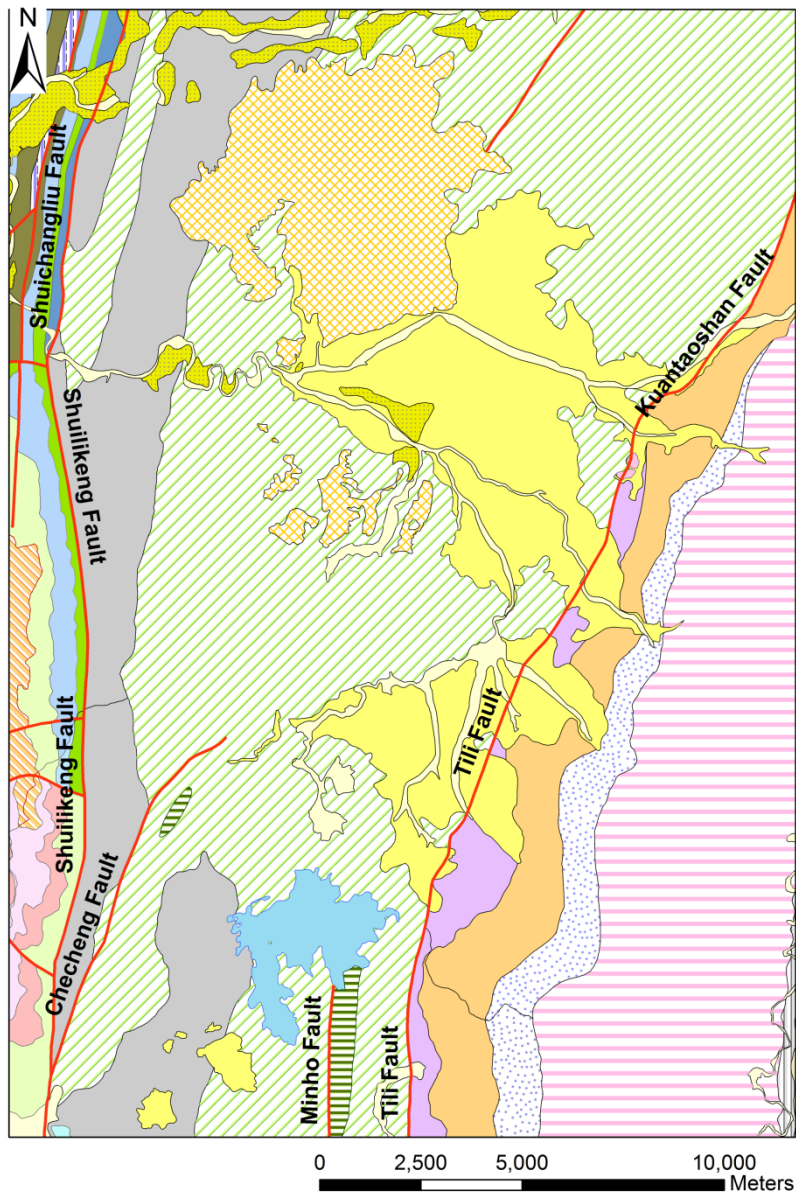
埔里盆地的重力低區

- 為深部堆積著密度較低的新世晚期-更新世初期地層(頭嵛山層)

Geological background



Geological background

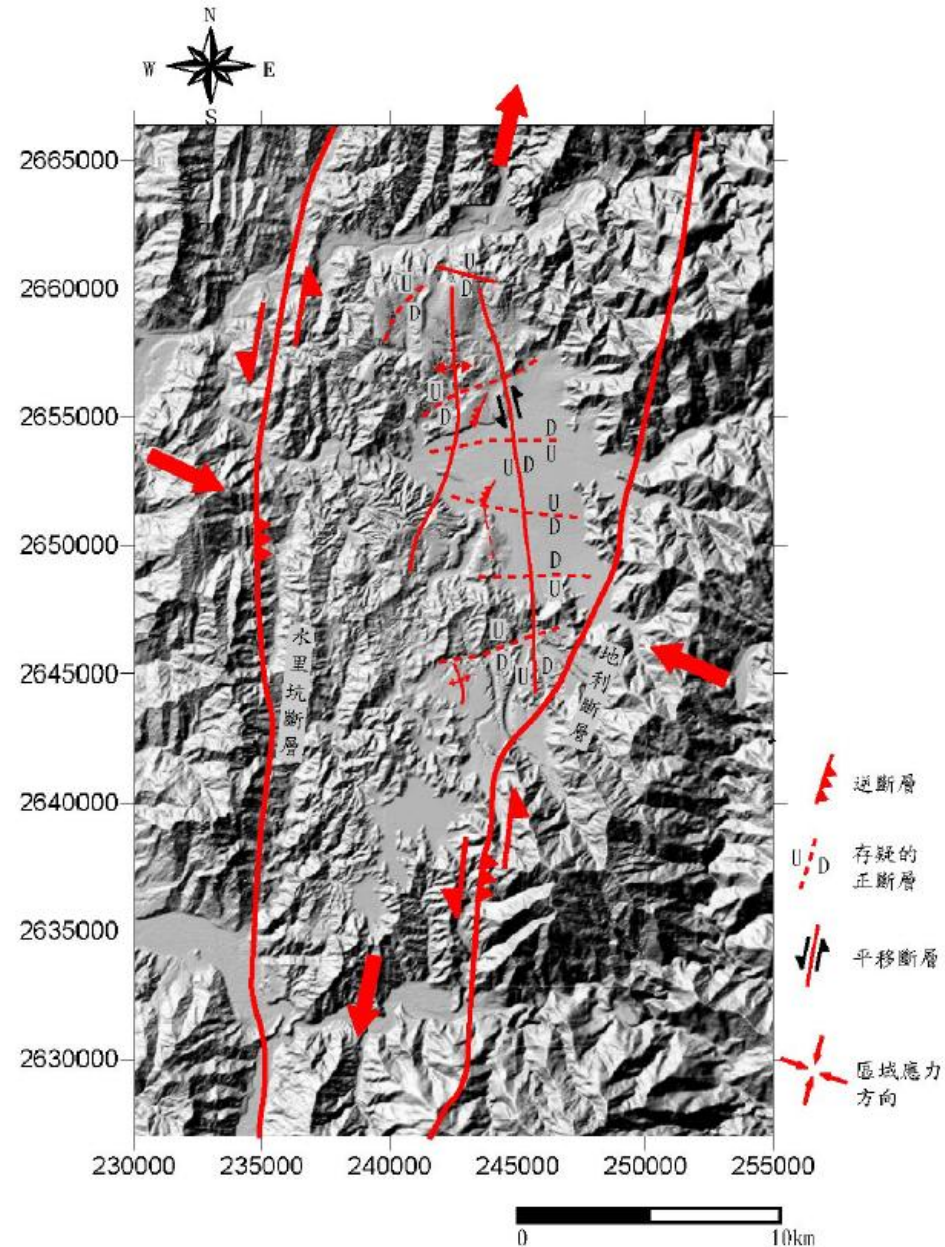


1. 史港溪斷層
2. 大坪頂背斜
3. 赤崁背斜及其東邊的逆斷層
4. 愛蘭逆斷層
5. 桃米坑背斜

(資料來源:中央地質調查所 流域地質圖, 2006)

盆地之成因

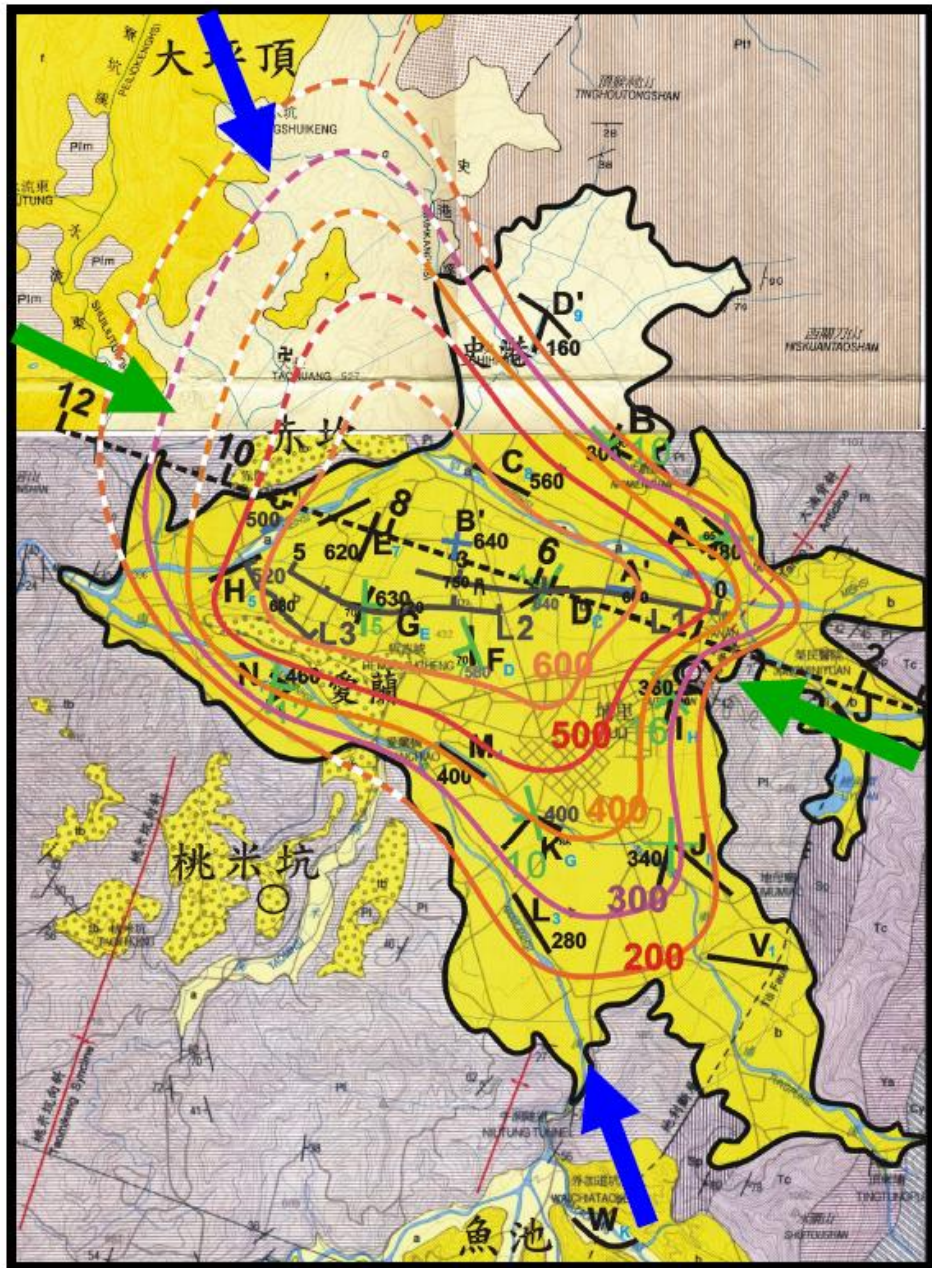
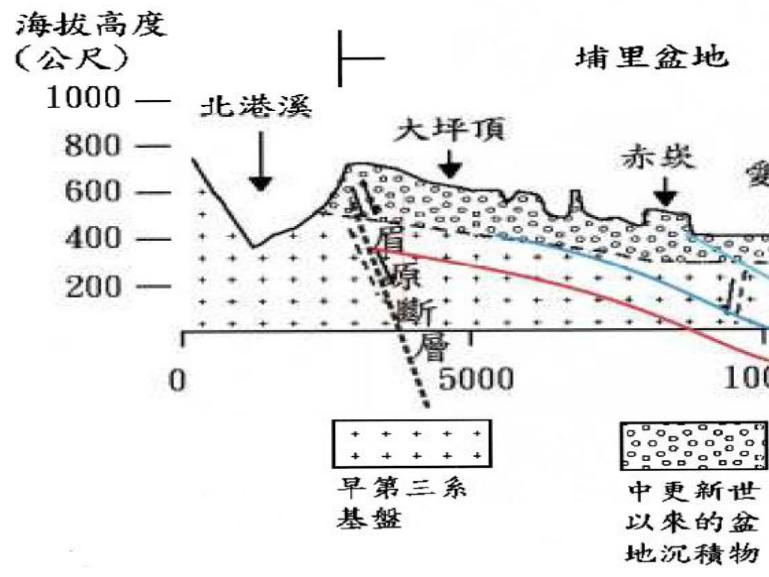
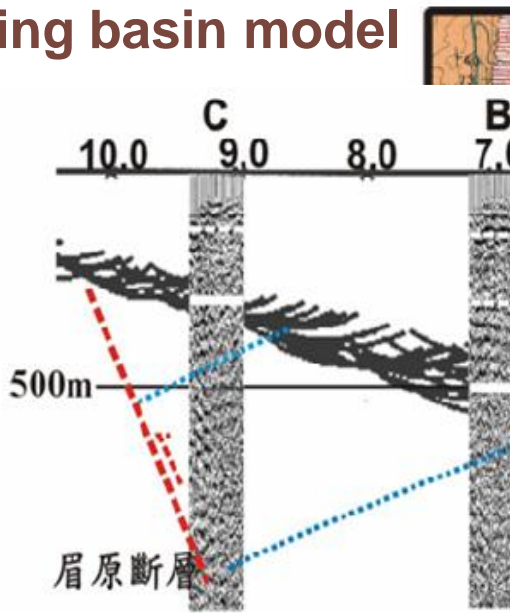
1. 曲滙作用(warping)及河流侵蝕作用
2. 背負盆地(piggyback basin)
3. 活動底脫斷層張裂沉陷形成
4. 雪山山脈內的橫移拉張造成 (Pull-apart basin)



Shallow Seismic Reflection result

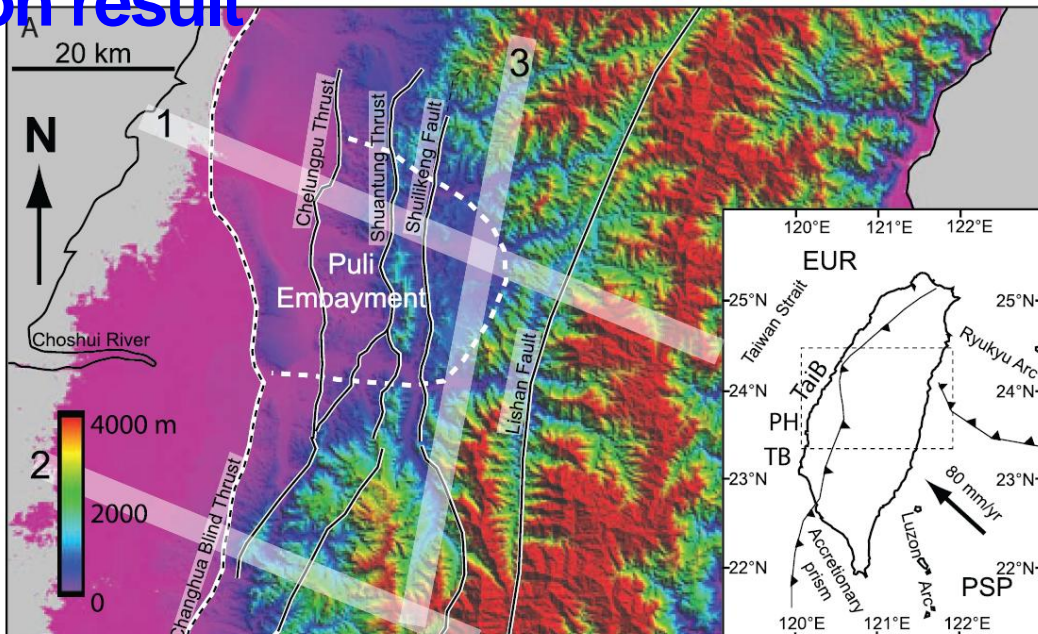
Down warping basin model

W

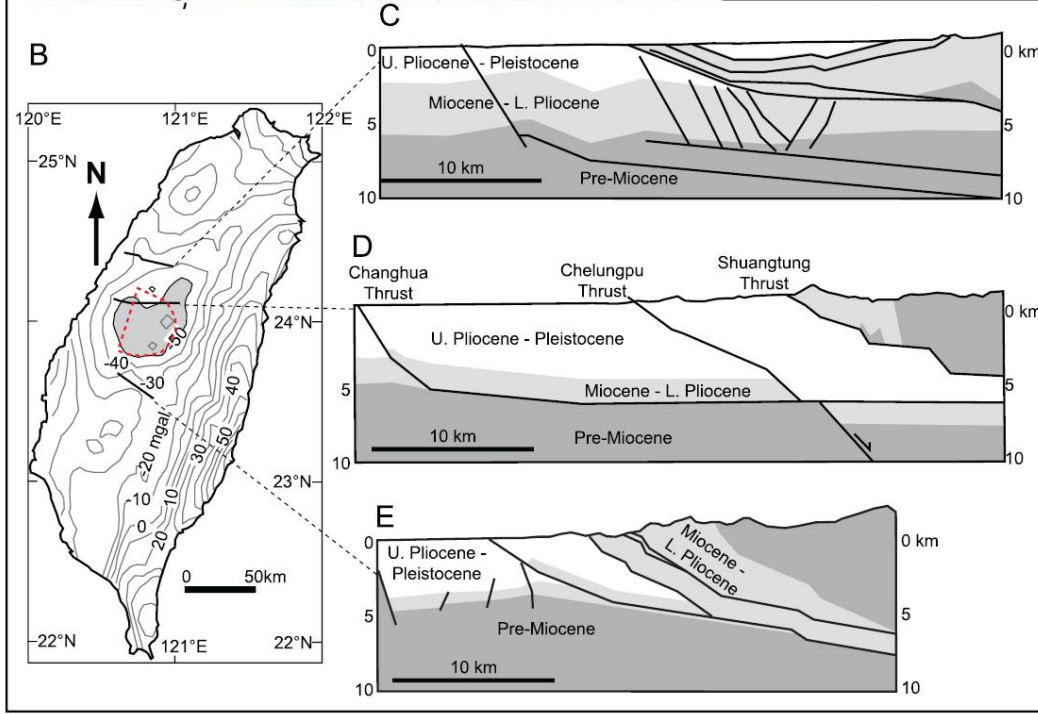


Shallow Seismic Reflection result

piggyback basin

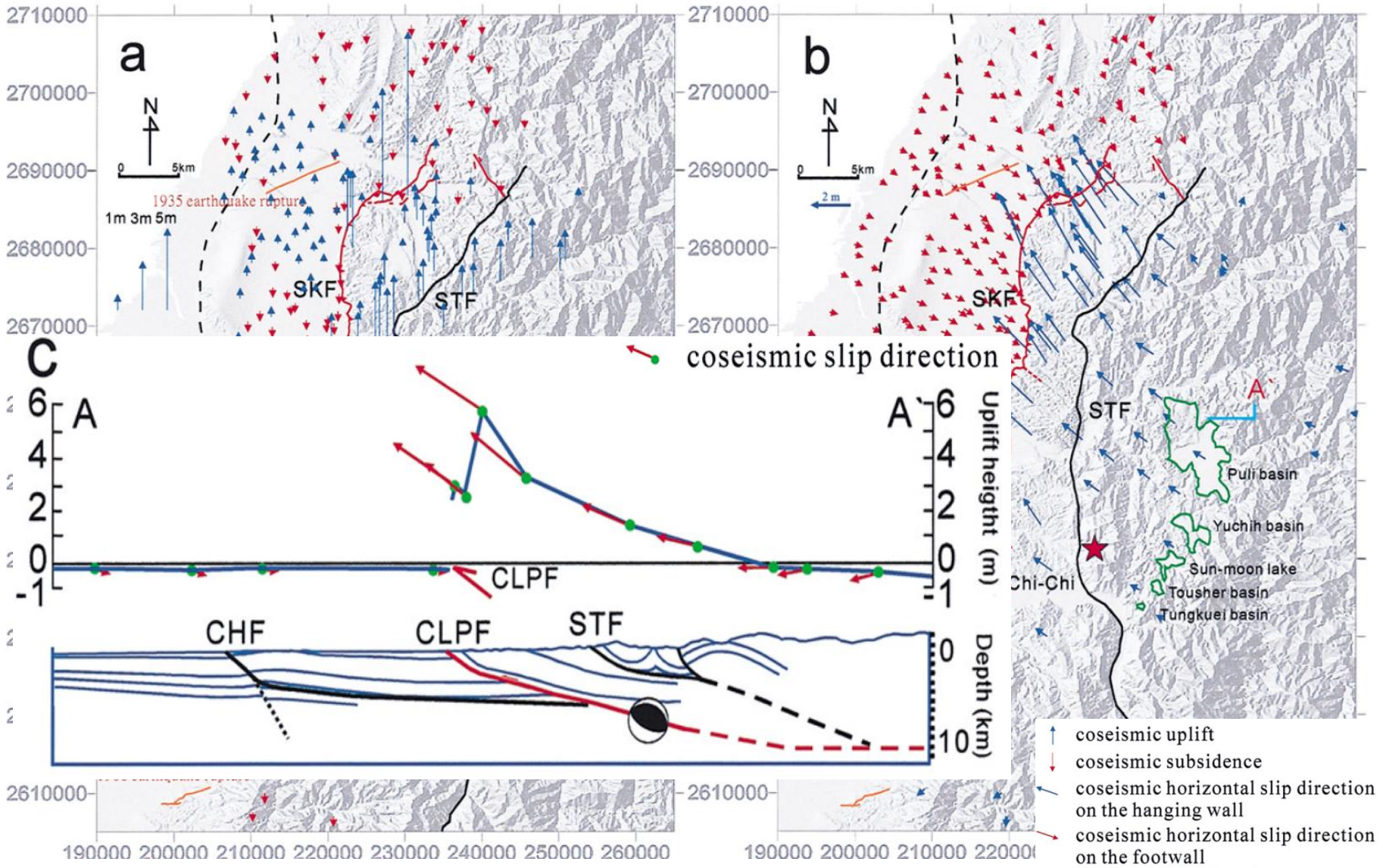


Bouguer anomaly map of Taiwan [after Yeh and Yen, 1992].



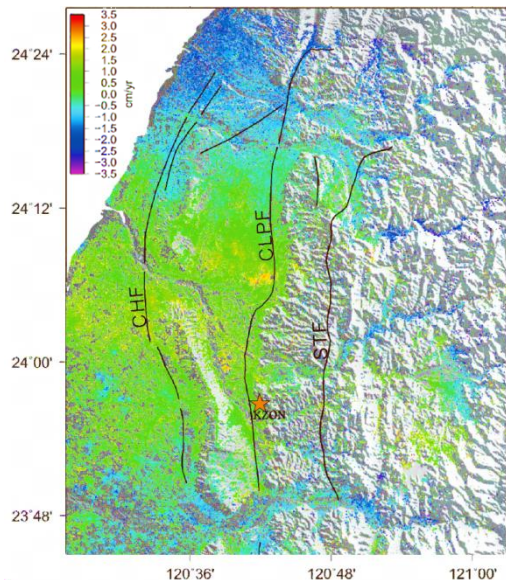
GPS measurements after the Chi-Chi earthquake

A detachment under the Puli basin caused the rifting of the basin

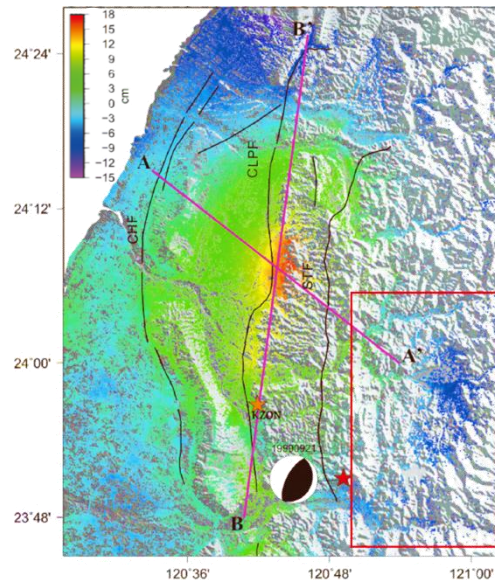


PSInSAR result

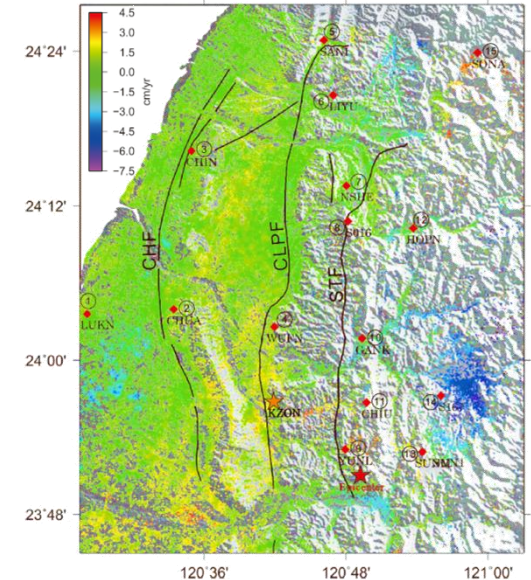
- There is small discrepancy between InSAR results and GPS measurements, however, the total deformation trends are very similar in the post-seismic period.
- Moreover, this study demonstrates that the capability of time series InSAR technique is not only good to monitoring the ground displacement in the subtropical area such as Taiwan, but also to analysis the long-term temporal and spatial deformation.



Pre-seismic Deformation

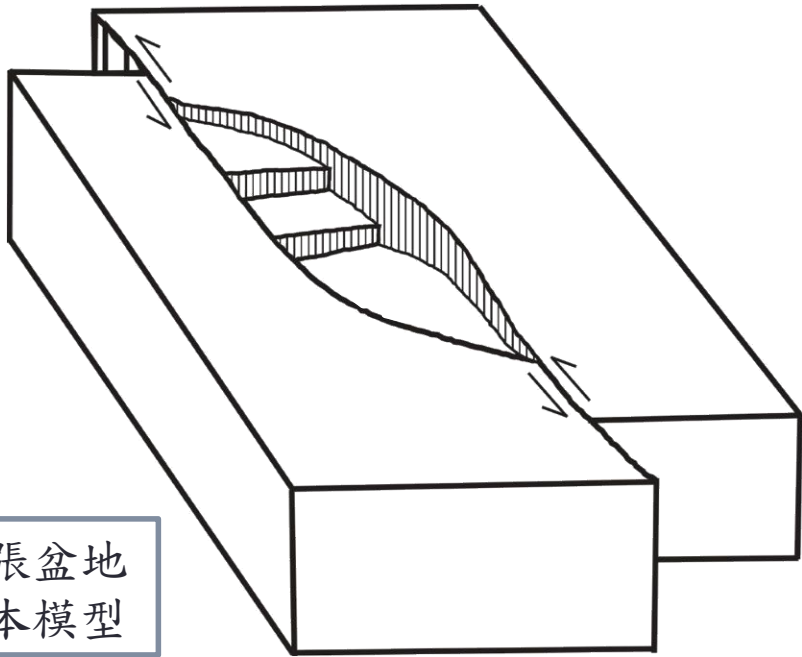


Co-seismic Deformation

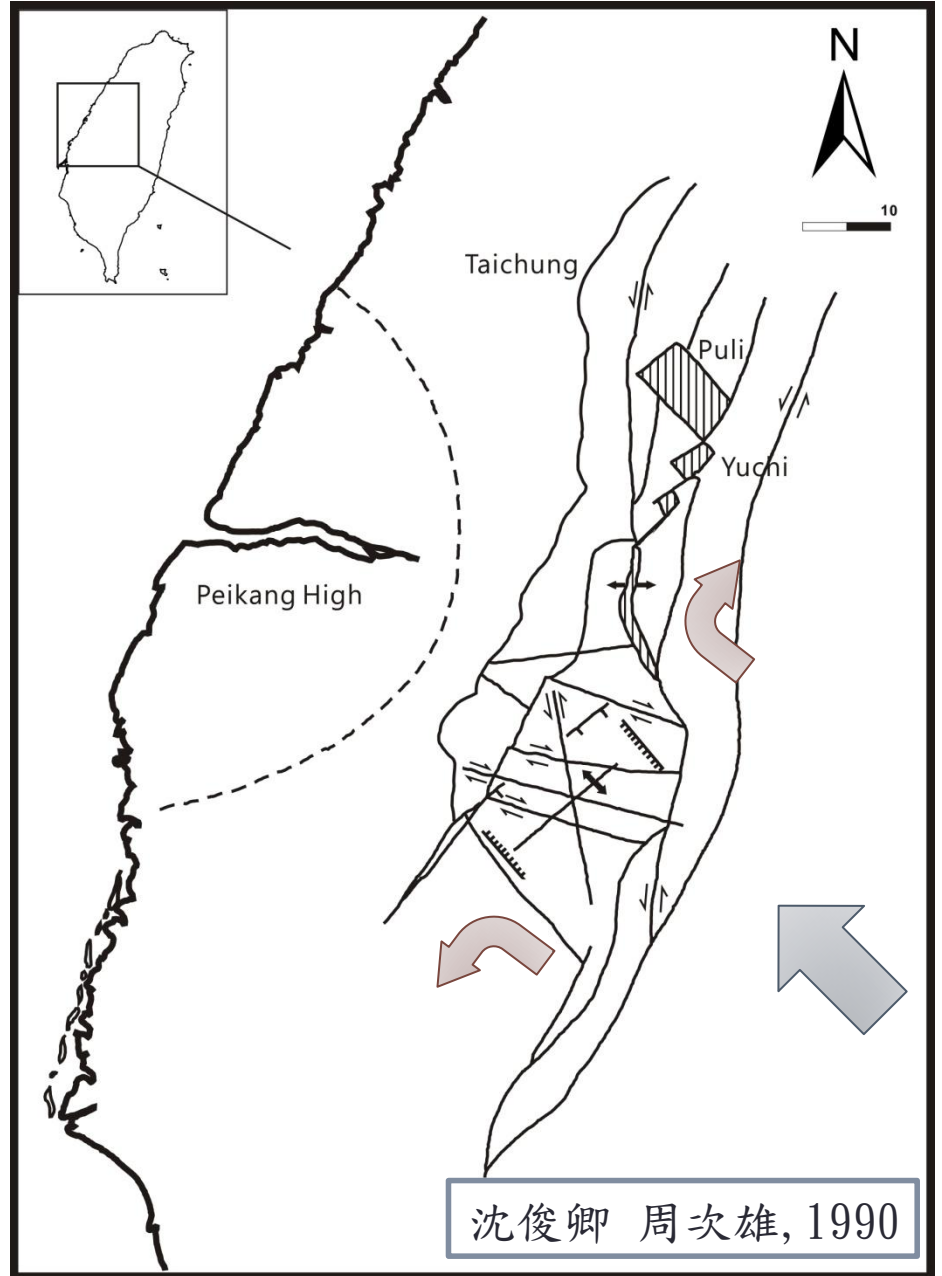
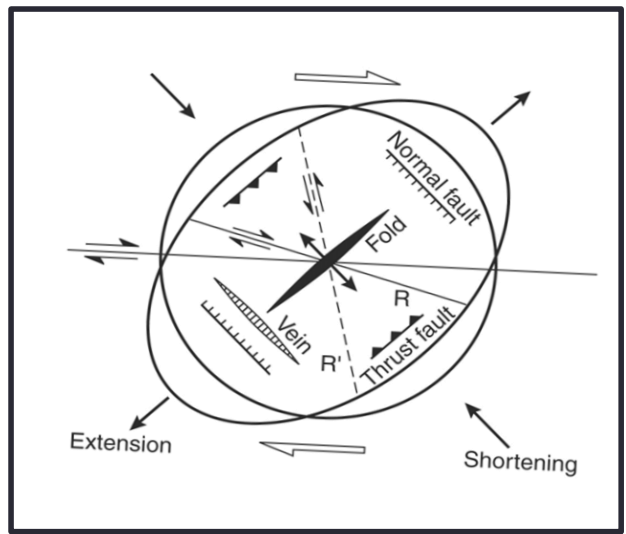


Post-seismic Deformation

Pull-apart basin

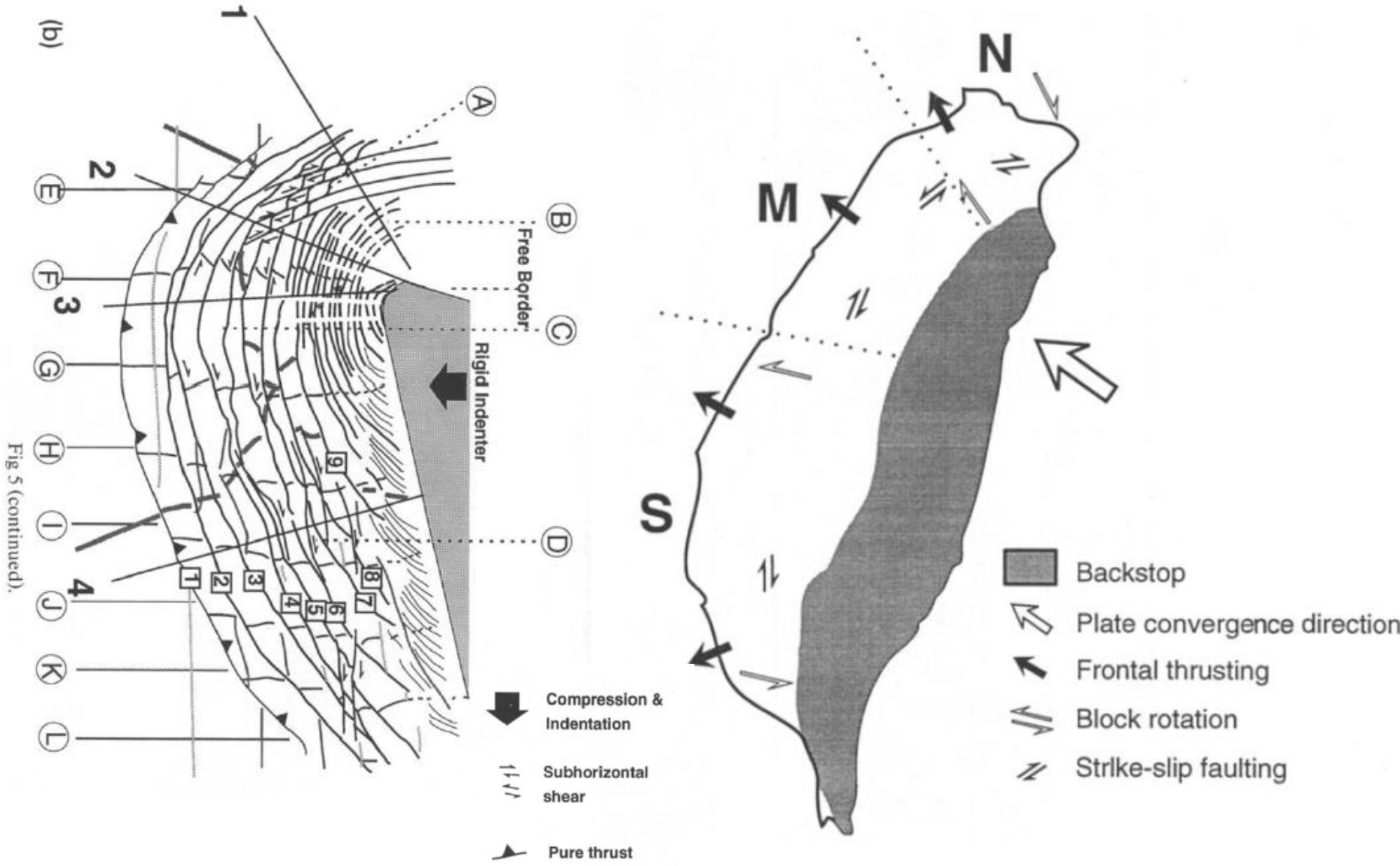


拉張盆地
基本模型

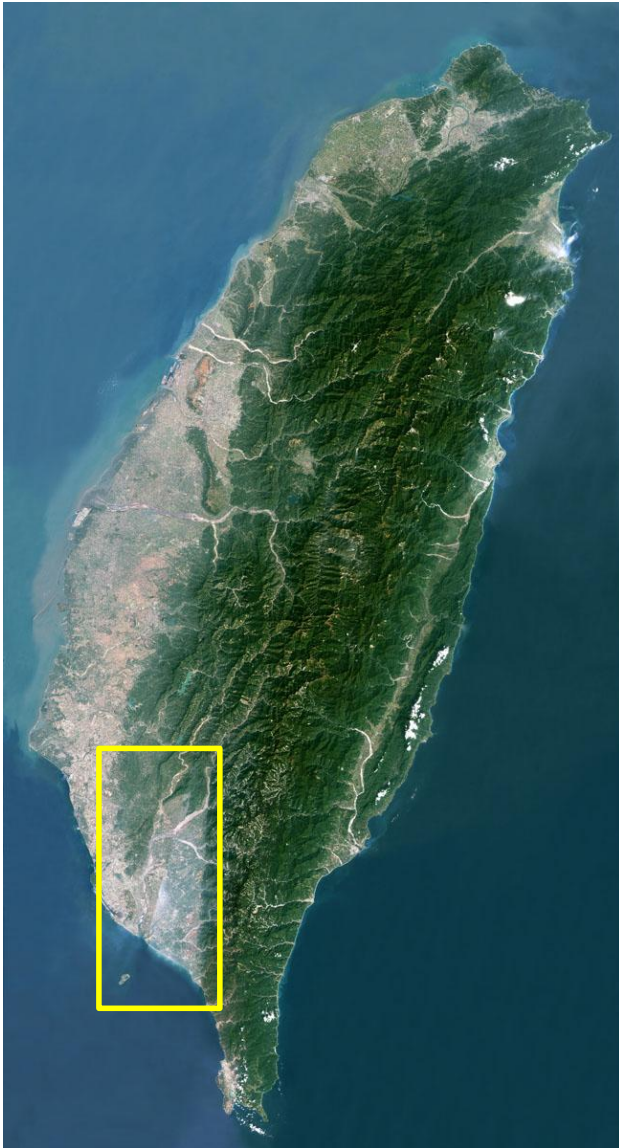


沈俊卿 周次雄, 1990

Oblique convergence, indentation and rotation tectonics in the Taiwan Mountain Belt: Insights from experimental modelling



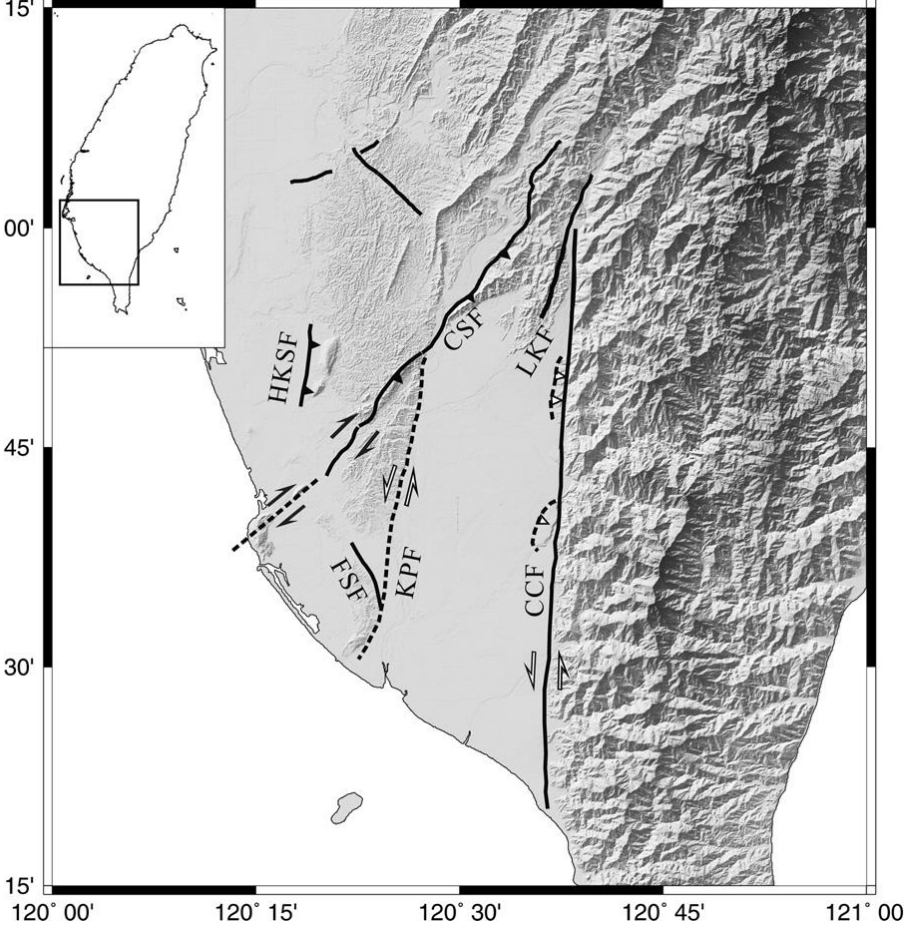
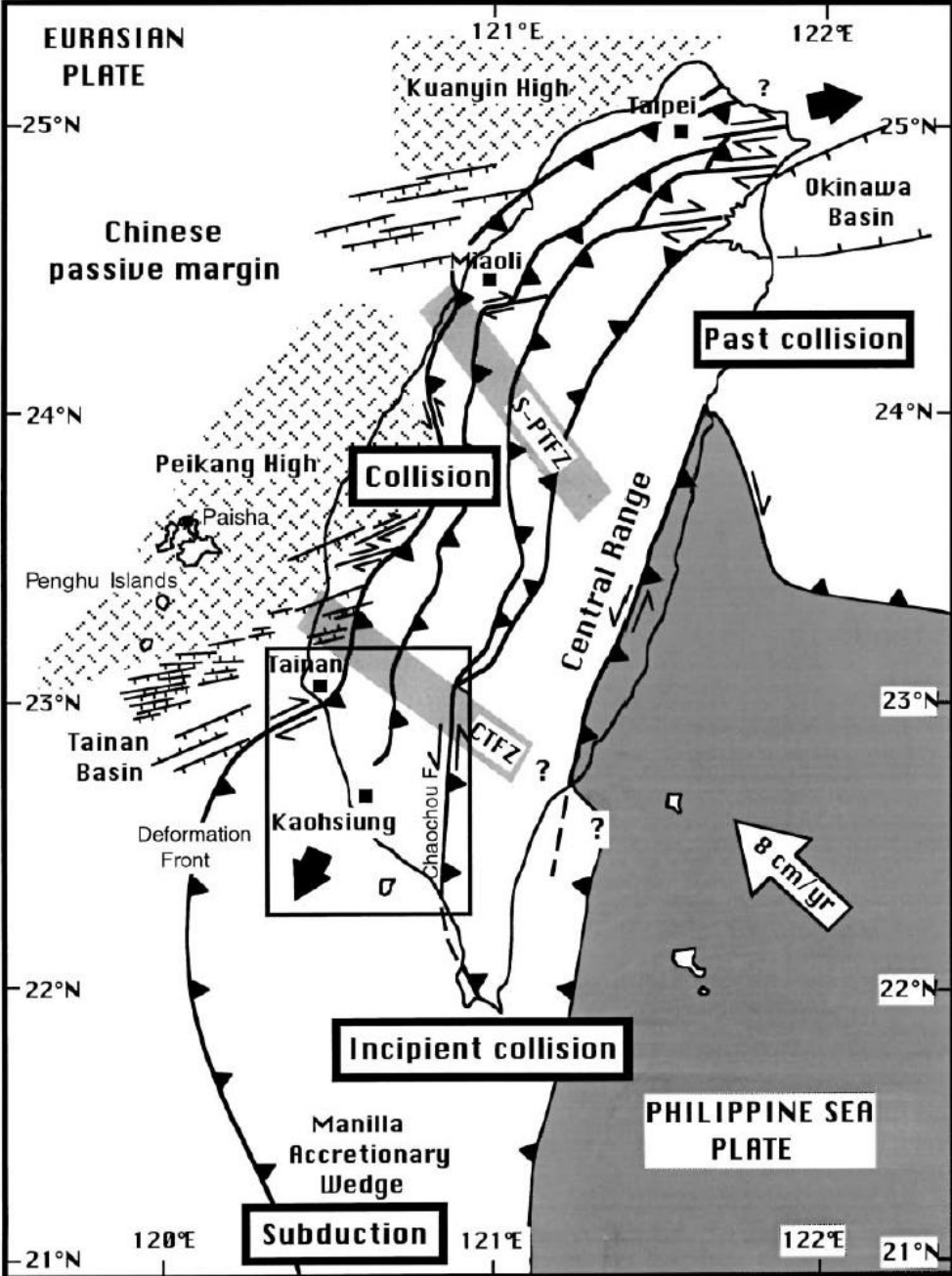
Pingtung plain



- 1210 Km² in area
- Triangular alluvial plain
- Tectonic escape or tectonic extrusion



Geotectonic setting

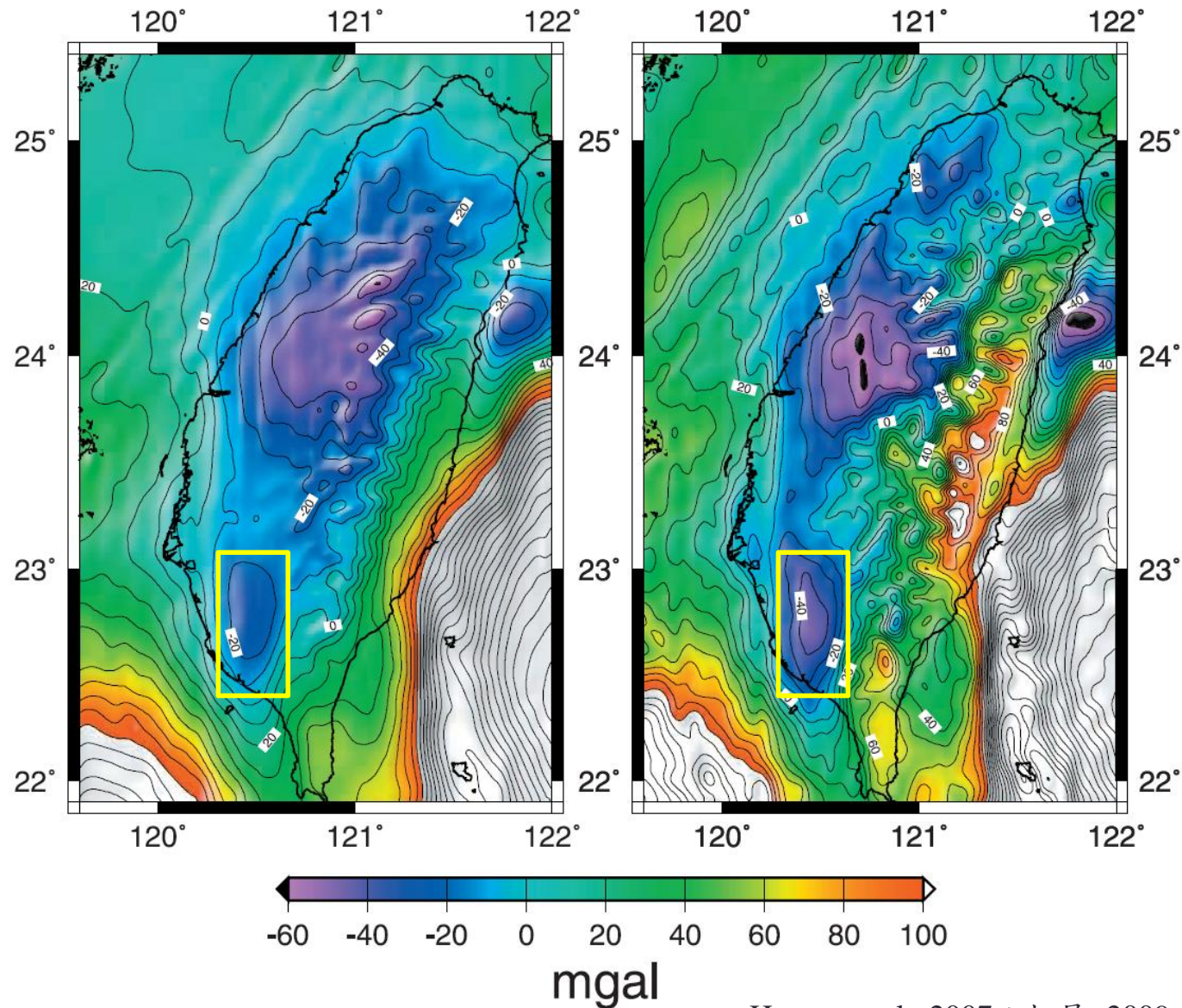


Lacombe et al., 2001

The Bouguer anomalies

At the flight altitude

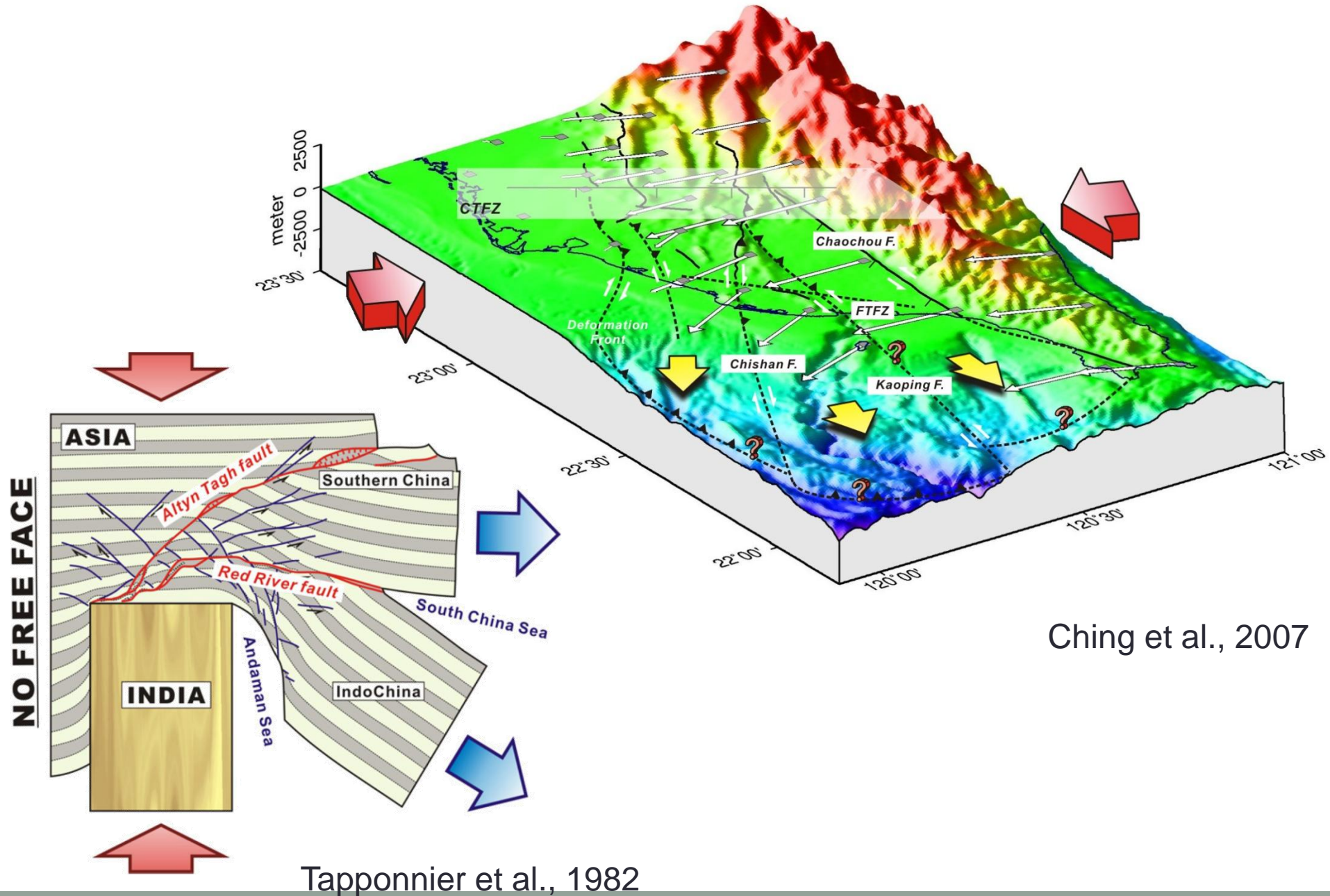
At sea level



屏東平原的重力低區

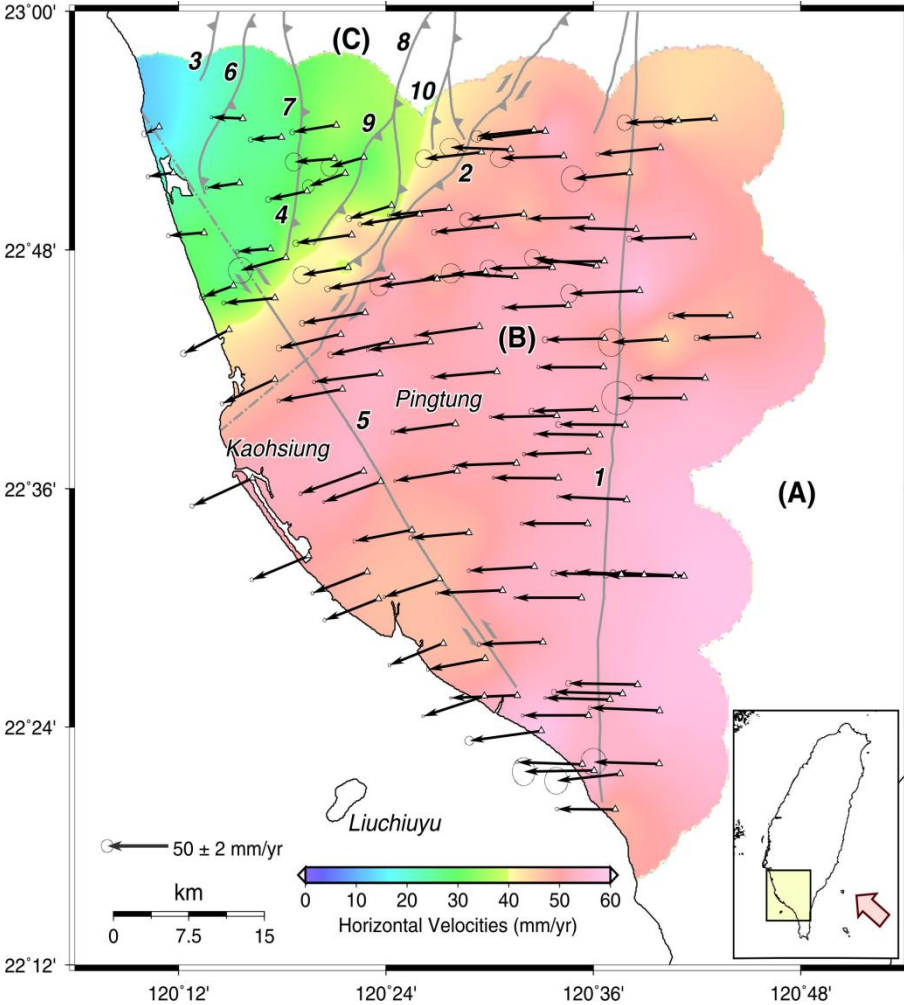
- 近地表厚層的沉積層所造成。

Tectonic escape or tectonic extrusion

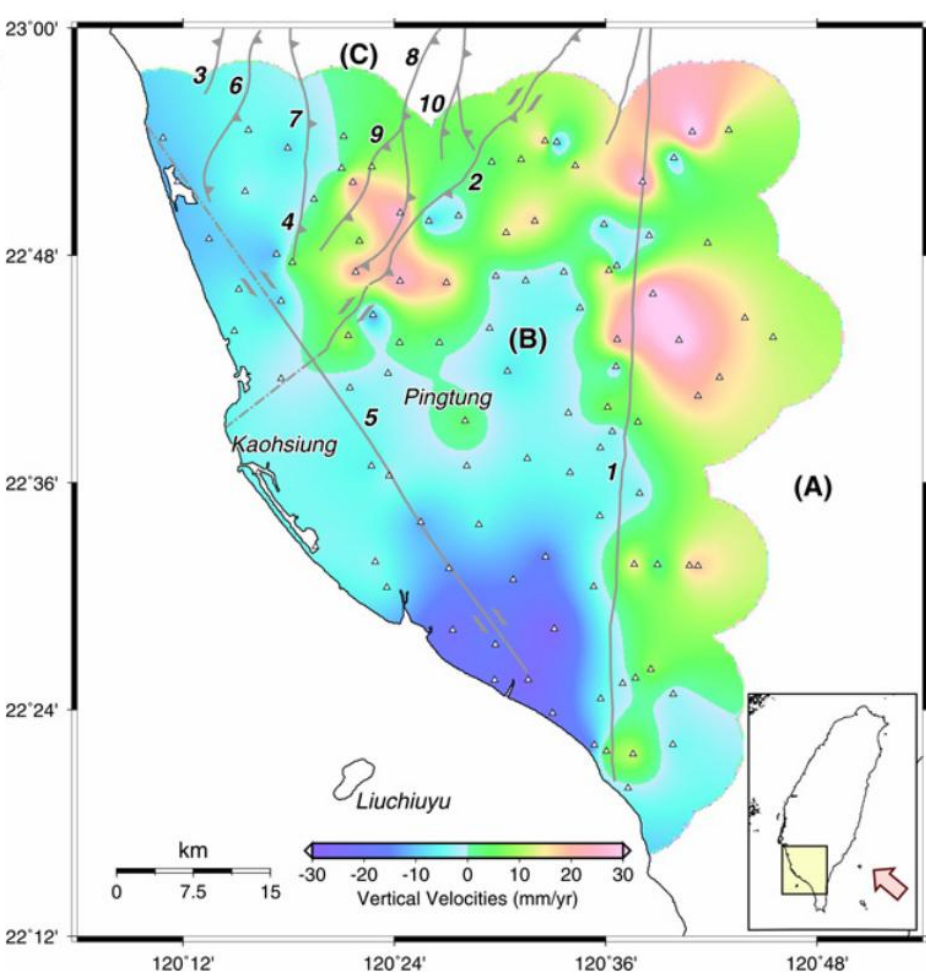


GPS measurements from 1995 to 2005

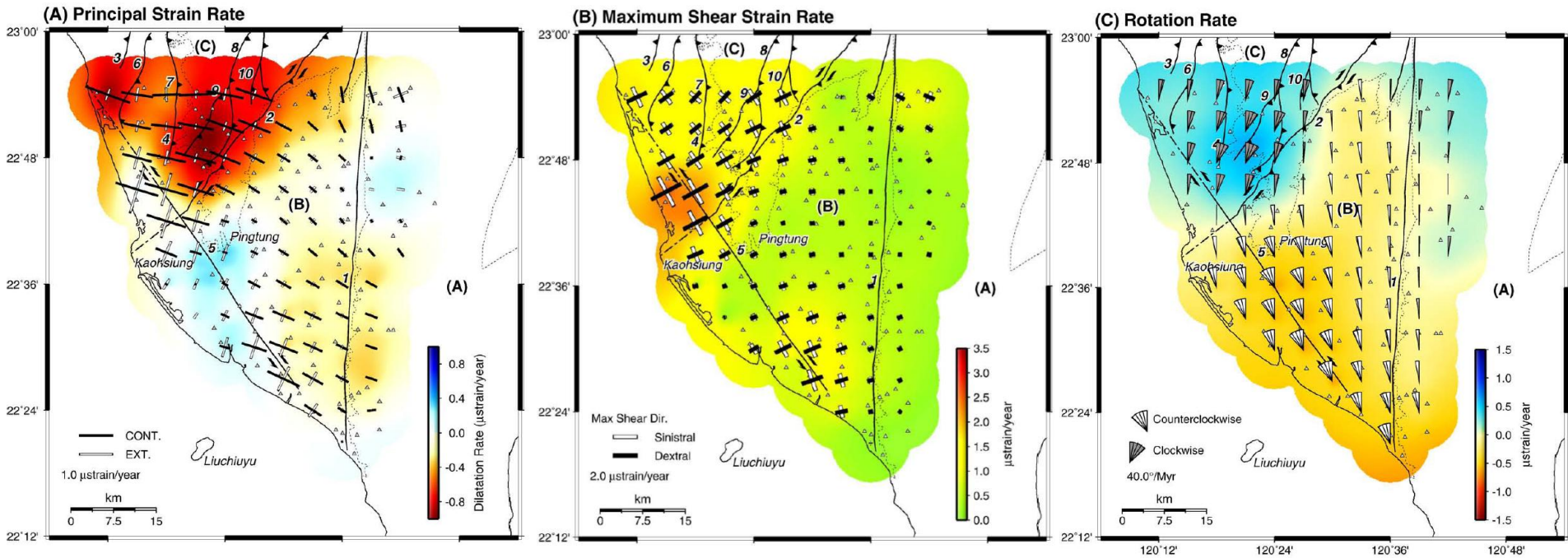
Horizontal velocity field



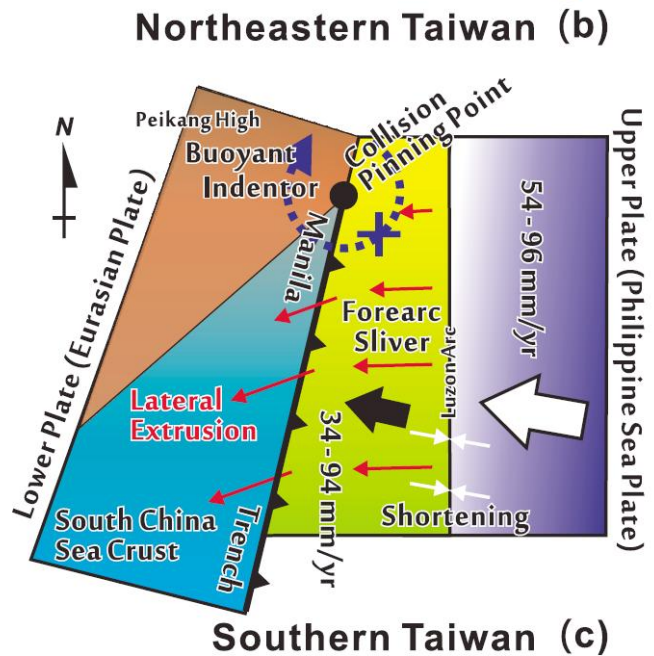
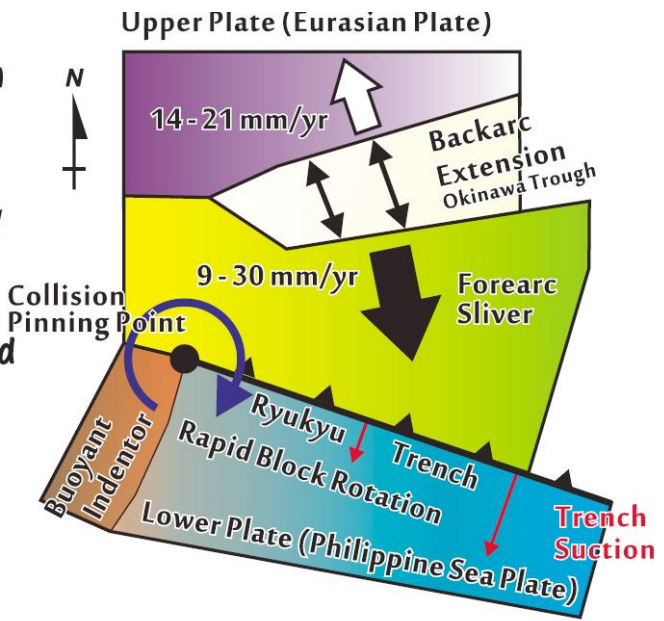
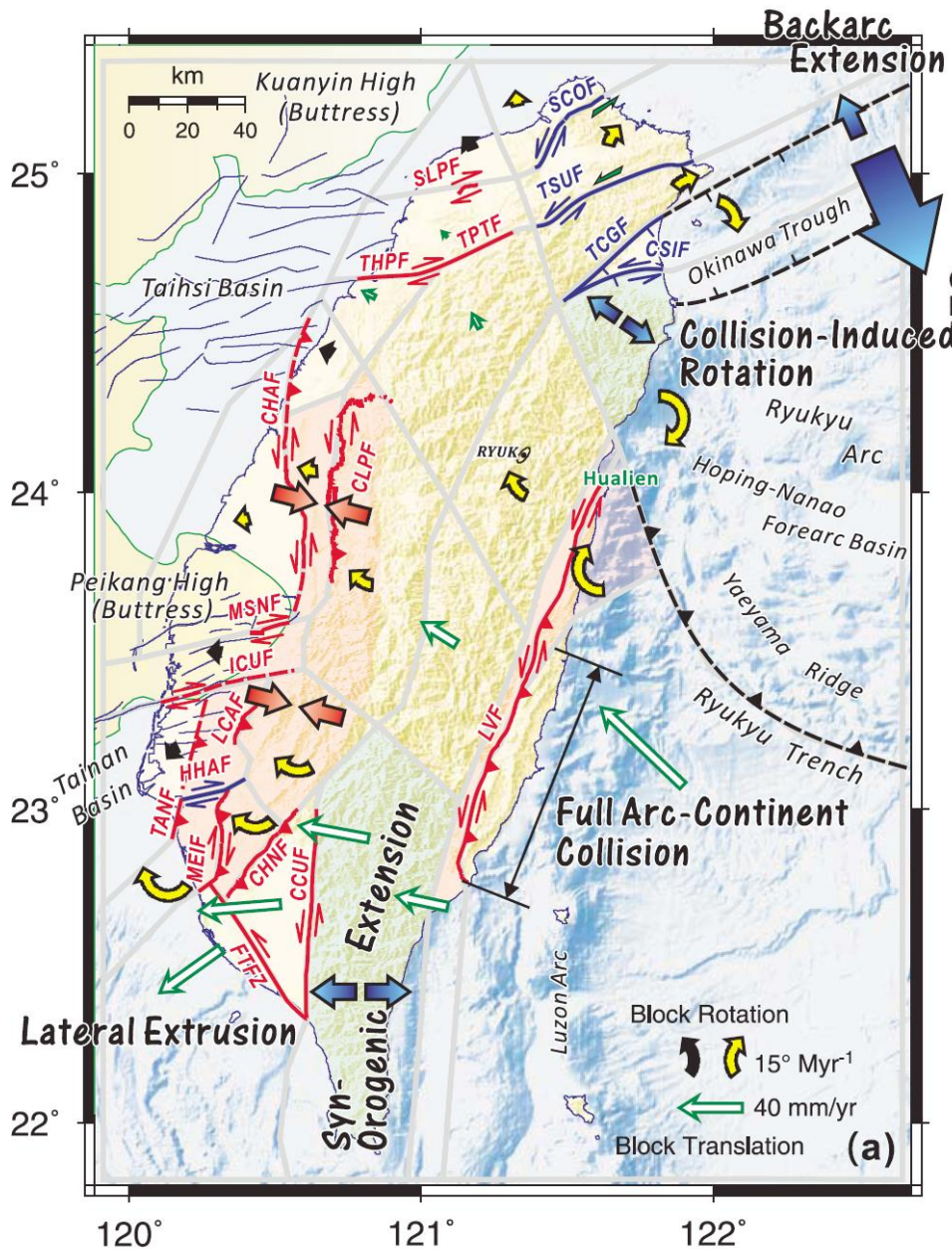
Vertical velocities



Distribution of strain rates in SW Taiwan

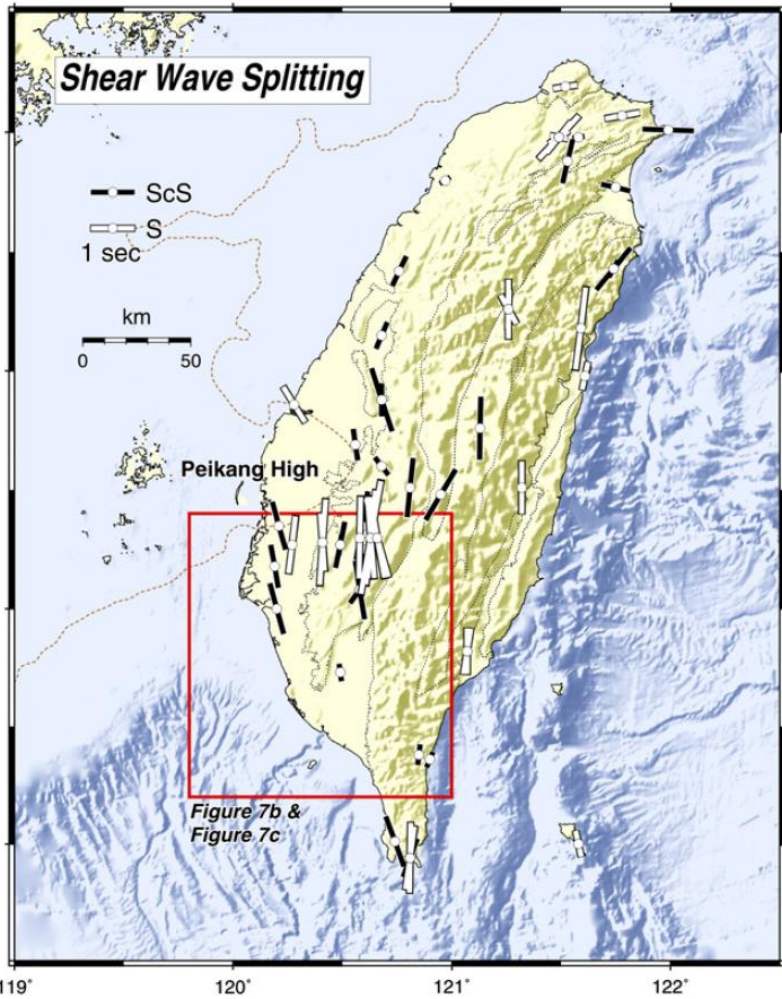


Schematic of the strain-partitioning model

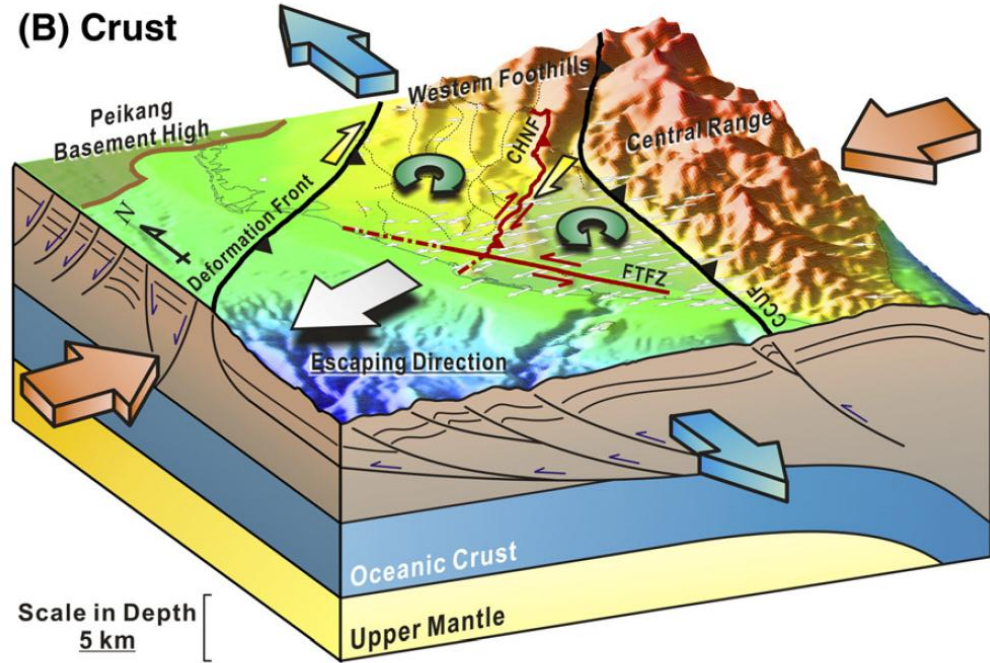


The tectonic kinematic model

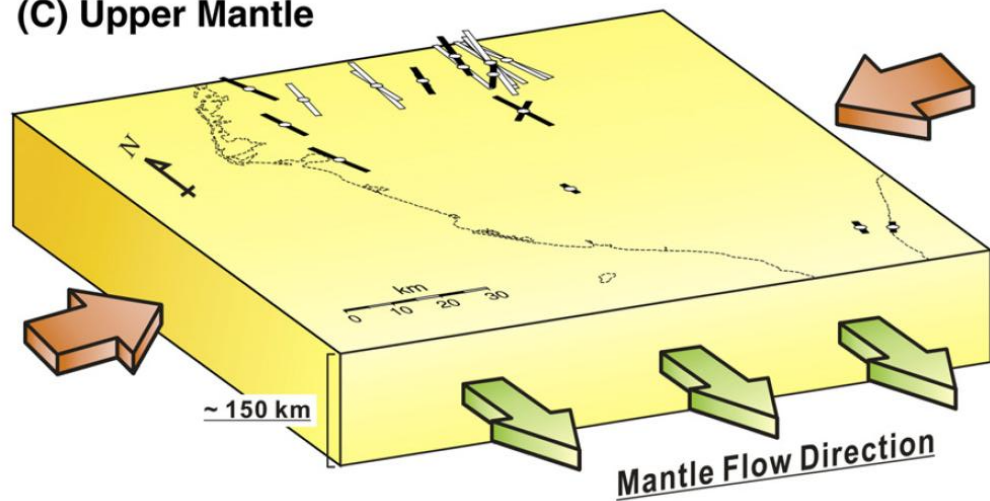
(A)



(B) Crust



(C) Upper Mantle



PSInSAR result

